USBM Contract No. G0122006

DEVELOPMENT OF TECHNIQUES AND THE MEASUREMENT OF RELATIVE PERMEABILITY AND CAPILLARY PRESSURE RELATIONSHIPS IN COAL

J. J. Taber
P. F. Fulton
M. K. Dabbous
A. A. Reznik

Department of Chemical and Petroleum Engineering
University of Pittsburgh

USBM CONTRACT FINAL REPORT (Contract No. G0122006)

January 21, 1974

DEPARTMENT OF THE INTERIOR
BUREAU OF MINES
WASHINGTON, D. C.

TABLE OF CONTENTS

TABLE OF CONTENTS
(Continued)

TABLE OF CONTENTS
(Continued)

ABSTRACT

Gas and water permeabilities of a large number of samples from the Pittsburgh and Pocahontas coals were measured at various overburden and mean flow pressures. A wide variation in the air and water permeabilities was obtained for each type of coal. Overburden pressure has the most significant effect on the single-phase permeability. Considerable hysteretic effect was observed for both air and water permeabilities. Gas permeabilities are affected to a lesser degree by mean flow pressures above atmospheric. However, at subatmospheric mean pressures, appreciable increase in permeability occurs for low permeability samples.

Air and water relative permeabilities were also measured for numerous samples of Pittsburgh and Pocahontas coals. Tests were performed under steady-state conditions for both drainage and imbibition cycles. Results indicate that the flow of gas is greatly reduced during the latter process, whereas it is largely undiminished over a wide water-saturation range during drainage. It is also shown that imbibition saturation distributions obtained from liquid-water imbibition as opposed to water-vapor adsorption produce gas permeability curves of radically different character. The effective permeabilities to both gas and water were significantly reduced with the application of overburden pressures in the range of 0 to 1,000 psig, but the general shapes of the relative permeability curves remained the same.

INTRODUCTION

The permeability of coal to gas and water is of interest to engineers in both the mining and petroleum industires. Much of the interest of the mining engineer stems from concern for the health and safety of the coal miner because the flow of methane into coal mines is one of the major causes of mine disasters in this country. Some deep mines produce 10 to 15 MMscf/D of methane and require the circulation of as much as 10 to 15 tons of air per ton of coal mined in order to clear the gas from the mine.[1] If this source of natural gas could be produced from the coal before the coal

is mined, it would help relieve the gas shortage as well as protect the safety of the coal miner.

In recent years a number of petroleum companies have shown an interest in coal as a primary energy material that can be converted into electrical energy or into gaseous and liquid products. Both above and below ground processes are being studied intensively. Knowledge of the basic permeability and relative permeability of coal to gas and water should be very useful to petroleum engineers contemplating these new processes for the conversion of coal into a form of energy suitable for the consumer.

By petroleum standards, the literature on the gas or water permeability of coal is rather limited. Gas permeabilities reported in the literature range from near zero to at least 1,890.49 md. However, most of the reported permeability values for all except the Middle Kittaning coal are very low, with values above 10 md being unusual.[2] Previous work also indicated that the coal permeability is very sensitive to different confining pressures used during the flow measurements.[3]

The permeability of coal to water has been measured by several workers, and effects not normally observed in petroleum bearing rocks have been reported.[4-6] A discussion of the previous water permeability work is presented with the results on water permeability.

Porous rocks generally possess a fairly homogeneous structure and, therefore, small permeability variations with in the porous body. It is sufficient to measure the permeability of only a few core samples to obtain a representative permeability value for the porous rock. Coal, on the other hand, possesses a fracture network consisting of systems of micro and macro fractures in addition to submicroscopic intergranular pore spaces. Because of this inherent complex structure, local variations in permeability are quite significant. Thus, measurements on a large number of samples are required to establish a permeability distribution and possibly find a mean absolute permeability representative of a large section of a given type of coal. Part I of this report presents the results of a number of permeability measurements under various conditions. The relative permeability results are given in Part II and the capillary pressure results in Part III.

APPARATUS

The experimental apparatus used in this work made it possible to measure the single-phase gas or water permeabilities of coal samples as well as the relative permeabilities to gas and water during simultaneous two-phase flow experiments. A Core Labs micropermeameter was made an integral part of the flow system. A flow diagram of the apparatus is shown in Figure 1. The main constituents of the apparatus are (1) a constant pressure, constant flow rate gas injection system, (2) a high precision, constant flow rate. positive displacement Ruska pump for fluid injection, (3) a stainless steel Hassler-type core holder capable of handling pressures up to 1,000 psig and (4) a gas-liquid separator, a graduated fluid receiver tube and gas flow metering equipment.

The downstream gas flow rate was measured by calibrated orifices and a soap bubble tower. A Millipore filter was inserted in the fluid injection line to control any possible plugging of the coal samples by bacteria in the distilled water.

To study the effects of gas slippage on the permeability of coal, an extended mean pressure range permeameter (Figure 2) was set up. With this permeameter, both negative and positive pressures could be obtained and regulated at the upstream and downstream ends of the sample. As a result, mean flow pressures below atmospheric and $1/P_m$ values > 1 could be obtained conveniently.

Water permeabilities were also determined at constant pressure differentials using a constant head gravity feed system. The constant low pressure head of approximately 0.5 psig was maintained by the use of a drip feeder arrangement. During the flow tests the samples were confined in the rubber sleeve of the Hassler holder under controlled external pressure from a high pressure source.

SAMPLE PREPARATION

Unlike most porous rocks, coal is highly friable and disintegrates into fragments upon the application of a pressure force or a shearing stress. Because of the inherent structure and texture of coals, the problem of obtaining reasonable core samples becomes a difficult one. Thus, the standard techniques used in coring oil reservoir rocks had to be revised for the present study.

Two types of coal were received for this investigation. These were samples from the Pittsburgh and Pocahontas coal seams. The two types represented two extremes: a friable Pocahontas coal and a less friable, fairly solid Pittsburgh coal.

The first step in the sample preparation was to cut flat surfaces across the fresh coal chunks in a direction perpendicular to the bedding planes with a 14-in. diamond blade. For the flow tests, cylindrical core samples were desirable because most core holders are designed to hold and seal cylindrical core plugs. Whenever possible these cylindrical cores were drilled along the bedding planes with a 1½-in. diameter diamond dust core bit. Such cores had to be drilled with extreme care and with minimum lateral vibrations. The external surface of some of these samples had to be smoothed by coating the surface with a very thin layer of epoxy. This was necessary to avoid rupture of the sleeve of the core holder at high confining pressures. The top and bottom faces of the sample were smoothed to flat parallel surfaces with a surface grinder exerting the minimum pressure on the sample while grinding an even surface.

The routine of obtaining several sets of measurements on some samples at various overburden pressures increased the likelihood of sample failure. The possibility of structural collapse was minimized by encasing the samples axially in an undersized pliable rubber sleeve. The sleeve fits snugly around the core and its thickness of under 1/16 in. allows only slight compressibility. Thus, the overburden pressure can be transmitted without appreciable reduction.

Very friable samples were carefully cut with a hand saw and mounted in silicon rubber holders. The silicon rubber used was a 3120 Dow Corning encapsulant.

Before measurements were made, the samples were dried in a vacuum oven at 80°C for a period of 24 hours. Higher drying temperatures have adverse effects on the flow properties of coal.

WATER SATURATION OF COAL SAMPLES

For the water permeability tests, saturation of the coal samples to 100 percent with water was accomplished by placing the samples under a strong vacuum for a period of 6 hours and then allowing the evacuated samples to imbibe distilled water for 48 hours.

It was found that coal continues to imbibe water at a significant rate for a considerable length of time. This was true for samples that were placed under vacuum prior to the admission of water as well as samples that had been just air dried and then soaked in water. Table 1 shows that the sample continued to take up moisture for more than 160 hours. If the gain in weight is plotted against time as in Figure 3, it appears that most of the gain in weight is completed in 2 days. It is obvious that a lower water porosity will be reported if the sample is placed in water for a short time. However, it is doubtful if any of the additional water that is imbibed after 2 days will contribute to flow. For this reason, a saturation time of 48 hours was arbitrarily set for the pore volume determination and for the 100 percent water saturation value.

EXPERIMENTAL RESULTS

PART I - THE PERMEABILITY OF COAL TO GAS AND WATER

Gas Permeability of Coal

Measuring the absolute permeability of coal is a first and necessary step for the study of the two-phase relative permeability characteristics. The absolute permeability to air of 35 samples from the Pittsburgh coal are reported in Table 2. For each sample the permeability was measured at various mean pressures within the range that could be obtained with the permeameter and then extrapolated to infinite mean flow pressure. All measurements were made at the same overburden pressure of 200 psig since this was found to have the most significant effect on the permeability of coal, as will be discussed in a subsequent section. The measured permeabilities for the Pittsburgh coal varied from essentially 0 to 50 md. Most samples, however, had permeabilities to air below 10 md and approximately 50 percent of the samples had permeabilities between 0.1 and 10 md. For the friable Pocahontas coal, absolute permeabilities to air in excess of 100 md were encountered. The data again indicated a wide spread in permeability in a fashion similar to the Pittsburgh coal. Because of this wide variation in permeability, frequency distributions of the absolute permeability were established for both types of coal. These fractional distributions are given in Table 3. The permeabilities were grouped into the following categories: greater than 100 md, 10 to 100 md, 1 to 10 md, 0.1 to 1, 0.01 to 0.1 md and less than 0.01 md. The distribution for the Pocahontas coal was established from measurements made on 28 samples. It indicates that, although a few samples of this friable coal had permeabilities greater than 100 md, the permeability of 60 percent of the samples was found to be between 0.1 and 1.0 md. Table 3 also shows the effect of overburden pressure on the distribution for the Pocahontas coal. When this pressure increased to 400 psig, no samples had permeabilities above 100 md and the permeabilities of a few samples dropped to the range below 0.01 md. Figures 4A and 4B are histograms comparing these distributions for the Pittsburgh and Pocahontas coal at the same external pressure and for the Pocahontas at two different pressures.

Effect of Mean Flow Pressure

Darcy's law does not account explicitly for the mean flow pressure, with the exception of the volumetric gas flow rate that has to be determined at the average flowing pressure. The well known Klinkenberg effect[7] indicates that the gas permeability of porous medium is a linear function of the molecular mean free path. As a result, the permeability of a porous medium to gas varies for each gas and with the mean pressure at which gas flows through the medium.

The effect of mean flow pressure on the permeability of coal was studied on 23 samples from the Pittsburgh and Pocahontas coals. The great differences in permeability between separate samples from the same coal (and even from the same lump) required that many tests be made to establish tentative relationships with confidence. The permeabilities of the samples covered a wide range - from 0.05 md up to 250 md for some Pocahontas coal samples. Most of the samples were dry except for a few that contained some moisture. The overburden pressure was maintained constant at 200 psig in all tests. The flowing medium was air and the reciprocal mean flow pressure, $1/P_m$, varied between 0.5 and 5.0 atm^{-1}. It is evident that values of $1/P_m > 1$ correspond to sub-atmospheric mean flow pressures.

The unique behavior shown by Figure 5A is typical of all coal samples with low permeabilities (below 10 md). Invariably, three straight-line segments could be drawn through the data points for those samples. Starting at high average pressures and moving in the direction of decreasing mean flow pressures (increasing $1/P_m$), the permeability first increased at a certain rate that was different for each sample. When P_m dropped below atmospheric, the permeability increased at a much faster rate defining a second straight-line segment. However, at lower mean flow pressures (below 0.5 atm) the rate of permeability increase was much smaller, marking a third line segment. The slope of the third segment was always less than that of the first and the second and was even horizontal in some cases.

The rapid increase in permeability was lessened by the presence of moisture in the samples as indicated by Figure 5B. The unique behavior (i.e., the three-segment Klinkenberg plot) was not observed for the coal samples having a high permeability. Figure 5C shows that a single straight-line segment relates the gas permeability of this permeable coal sample to the reciprocal mean pressure over the entire range of $1/P_m$.

Table 4 contains a listing of the permeability of some Pittsburgh coal samples at an average flow pressure of 1 atm and the permeability of the same samples extrapolated to infinite mean flow pressure ($1/P_m = 0$). Except for Samples PGH-6, 10 and 14, the reduction in gas permeability at $P_m = \infty$ is less than 20 percent of the magnitude of the permeability at $P_m = 1$ atm. Thus, increasing the mean pressure above atmospheric appeared in most cases to have little effect on the permeability of coal to gas. However, significant increases in permeability do occur if the mean pressure can be reduced to values somewhat less than 1 atm. Additional permeability measurements at various mean flow pressures are reported in the Masters thesis produced by Sunil B. Lal and Ismail Talaat while working on this project.[22,23]

Effect of Overburden Pressure

A series of tests were made to study the effect of overburden pressure on the permeability of coal. Samples from the Pittsburgh and Pocahontas coal were subjected to pressure cycles of loading and unloading and the permeability was measured at each point of the stress cycle.

Overburden pressures were simulated by applying an external gas pressure on the stainless steel Hassler-type core holder. This creates a radial stress field that is axially isotropic. A small element of coal in a coal formation experiences in-situ a stress field that is spherically isotropic. The radially applied pressure results in greater deformation of the internal structure of coal than that caused by a pressure field that is equal in all directions. As a result, the external sleeve pressure on the holder is approximately equivalent to twice that value in overburden

pressure.[8] For a fractured system such as coal, this estimate seems to be conservative.

The permeability of coal samples was found to be extremely sensitive to the overburden pressure and was drastically reduced as this pressure increased. Figures 6 and 7 are plots of the ratio of the permeability at a given overburden pressure, K_a, to the initial permeability of the sample at 200 psig overburden pressure prior to the application of any higher confining pressures, K_{ai}. The ratio K_a/K_{ai}, which is the fraction of the initial permeability, is plotted against the confining pressures for various consecutive stress cycles. This reduced coordinate for the permeability is very convenient for comparison of the behavior of samples whose initial permeabilities varied over a wide range.

The strong hysteretic behavior illustrated by Figures 6 and 7 for two Pittsburgh coal samples is typical of most samples studied. The fast rate of decrease in permeability with increasing overburden pressure is quite evident in both figures. At the maximum pressure attained, the slope of the loading curve is not zero, indicating that the permeability would be further reduced by an appreciable amount at still higher overburden pressures. The permeability increased along the unloading curve of the cycle, first at a very small rate that becomes increasingly higher at lower confining pressures. At the end of a stress cycle, the final permeability is considerably lower than the initial value at the same overburden pressure. However, these changes appeared to be time dependent as indicated by the small increase in permeability after 36 hours from the release of the stress.

By subjecting samples to various pressure cycles of loading and unloading, the permeability of a coal sample at any given confining pressure was found to be dependent upon the stress cycle as well. Figure 6 shows that the permeabilities of a sample at the highest overburden pressure attained in various stress cycles were almost identical. Also, the final K_a at the low pressure end of a cycle becomes increasingly closer to the initial value of that cycle as the number of the stress cycle increased. Above the second cycle the hysteresis loops became closed at both ends.

Figure 7 illustrates the behavior of a sample subjected to stress cycles with increasingly higher maximum pressure. Invariably, the tips of consecutive stress cycles fell on the extrapolated first loading curve. Thus, the first loading curve could be used to estimate the order of magnitude of the in-situ permeability of coal under the prevailing overburden pressure.

Table 5 is a listing of the permeability of fresh and prestressed samples from the Pocahontas coal at overburden pressures of 200, 400 and 1,600 psig, all taken on the loading curve. The second value at 200 psig is the final permeability at the end of the test. The permeability of the friable Pocahontas coal indicated a stronger dependency on the overburden pressure when compared to the Pittsburgh coal. In some cases, as with Sample 3, the reduction in permeability was so great that gas flow ceased at P_{ov} above 1,000 psig. A few samples even collapsed upon the application of higher overburden pressures.

The loading curves for 7 Pittsburgh and 8 Pocahontas coal samples were plotted on log-log coordinates. The region defined by K_a/K_{a_i} on such a plot for samples from the Pittsburgh coal is shown in Figure 8. The following approximate correlation may be used to estimate the order of magnitude of the in-situ permeability at a given overburden:

$$\log \frac{K_a(P_{ov})}{K_{a_i}} = - m \log \frac{P_{ov}}{P_{ovi}} ,$$

where $m = \begin{cases} 0.8 \text{ for Pittsburgh coal} \\ 1.0 \text{ for Pocahontas coal} \end{cases}$

K_a = gas permeability at P_{ov}, md

K_{a_i} = gas permeability at P_{ovi}, md

Permeability of Coal to Water

A large number of water flow tests were conducted on fifteen samples from the Pittsburgh and Pocahontas coals. Distilled water was flowed through the 100 percent water-saturated samples that were kept under an effective overburden pressure of 400 psig throughout most of the tests - except for those runs where the effect of varying the confining pressures was investigated.

The volumetric flow rates through the samples were measured at pressure gradients ranging between 0.5 and 5 atm/cm. To facilitate comparison between various samples, the water flux (apparent velocity of water flow), v, expressed in units of cc/sq cm·hr, was calculated and plotted vs the pressure gradient. Figure 9 is such a plot for a Pittsburgh coal sample (a) and a sample from the Pocohontas coal (b). In this case a linear relationship is obtained indicating a Darcy-type flow where

$$v = \frac{K_w}{u_w} \left(\frac{\Delta P}{\Delta X}\right).$$

However, in a few other cases the plots of v vs $\Delta P/\Delta X$ were not linear. The slope of the straight line is the water permeability, K_w, assuming that u_w is approximately 1 cp.

In previous laboratory experiments on the flow of water through Cwmtillery Graw coal,[4-6] it was reported that the water flow through the coal samples varied with time and eventually reached a steady-state flow rate in accordance with the relationship,

$$F = \alpha (1 - e^{-kt}) + \beta t,$$

where F is the total quantity of water that has passed through the specimen in time, t. The flow rate, Q, becomes

$$Q = \frac{dF}{dt} = \alpha K e^{-Kt} + \beta$$

so that for large values of t the flow rate becomes constant and equal to β. It must be realized, however, that all those water flow tests were conducted on dried coal samples that had not been water saturated prior to the tests. As soon as the dry coal samples are contacted with flowing water, imbibition of water by coal takes place and adsorption of water on the walls of the capillary flow passages results in their swelling. This progressive swelling effect, as water imbibition continues, causes blockage of a portion of the area of flow. When the imbibition of water reaches an equilibrium state, the flow rate reaches a steady value. Calculations based on Poiseuille's law for flow through capillaries indicated that an average of two-thirds of the cross-sectional area of the capillaries in the coal samples is gradually occluded during the regime of exponential flow.

It also appears that the critical concepts of relative permeability and that the permeability of a medium to a certain fluid must be determined at a 100 percent saturation of the fluid were either not known or were overlooked in those early studies.

The data reported[6] indicated a linear correlation between the steady-state flow rate and the flowing water pressure up to 600 psi (equivalent pressure gradient based on the dimensions of the samples used is 300 psi/in. or 8 atm/cm). However, because of a more rapid increase in water flow rate at higher pressure gradients, the authors suggested a nonlinear relationship of the form,

$$Q = A \log \Delta P.$$

We believe that the nonlinearity and the apparent increase in water permeability at very high pressure gradients reported by the authors resulted from the fact that the effective overburden pressure on the samples decreased as the flowing water pressure became high. In our water flow experiments, the confining pressure was increased as the pressure gradients were increased such that a constant effective overburden pressure was maintained all the time because the latter was found to have a significant effect on the permeability.

Comparison with Air Permeabilities

Here again, as with air permeabilities, a wide range in the water permeabilities of the Pittsburgh and Pocahontas coals was obtained. This is also consistent with previous results on the flow of water through Cwmtillery coal where variations of more than three orders of magnitude were reported for samples (2-in. cubes) that were visually similar.[6] However, no previous attempts were made to compare the water permeabilities of coal samples to their air permeabilities.

Table 6 contains a listing of the water permeabilities of Pittsburgh and Pocahontas coal samples as calculated from Darcy's law. Also reported are the air permeabilities of the same samples at a mean flow pressure of approximately 1 atm and 400 psig overburden pressure. The results indicate that for the Pittsburgh coal samples $K_w < K_a$ except for Sample 64 where $K_w > K_a$. It is true that $K_\infty < K_a$; however, the results of this work as well as those of others showed that mean pressure had little effect on the gas permeability of coal. For the friable Pocahontas coal, K_w was less than, equal to or greater than K_a. Many samples of this friable coal were internally fractured under the shear stress of the flowing water, resulting in higher water permeabilities. Samples with $K_w \leq K_a$ were obtained from relatively solid lumps of this coal.

Water Permeability Hysteresis

It was observed that the water permeabilities of coal samples consistently decreased in repeated runs. This is evident from the results of Figure 10. K_w is proportional to the slopes of the straight lines and these are becoming smaller in progressive runs. It is also evident that the relative change in K_w in two successive runs decreases as the number of runs increases. The second set of runs made on the same sample 2 weeks later and represented by the dashed lines on Figure 10 show that K_w of the second set falls within the range of the first set of runs. This variation in water permeability with history that was observed for many coal samples is clearly a hysteretic effect. As with gas permeability one should expect the water permeability of coal to

depend on the history and the confining pressure.

Effect of Overburden Pressure on Water Permeability

In this series of tests the water permeabilities were determined at constant flowing pressure differentials using a constant low pressure head flow system.

In general, K_w greatly decreased as P_{ov} was increased. At P_{ov} = 400 psig the water permeabilities of the coal samples were less than, equal to or greater than the air permeabilities. However, as the overburden pressure increased, K_w became always less than or equal to K_a. This was true for Pocahontas and Pittsburgh coal samples. In Table 7 the air and water permeabilities at various overburden pressures are reported for five coal samples.

The higher water permeabilities are attributed to the tendency of some samples to internally fracture by the flowing water at low confining pressures. This possibility was studied by conducting several experiments to determine if the coal samples would "fracture" or "pressure-part" if increasing pressure drops were applied, and if such pressure-parting did occur would it vary with overburden pressure. Figure 11 is representative of the results obtained. There is definite evidence of parting at a $\Delta P/L$ of about 0.4 with an overburden pressure of 100 psi. When the overburden was increased to 200 and 400 psi the samples did not fracture. This was true on all samples tested.

PART II - RELATIVE PERMEABILITY STUDIES

MEASUREMENT OF RELATIVE PERMEABILITIES

Most all of the effective and relative permeabilities to air and water were measured under approximate steady-state conditions by the stationary-phase method in which one of the fluids is immobilized within the sample by capillaric forces. However, a series of runs was conducted on a sample of Pittsburgh coal where gas and water relative permeabilities were determined by the Penn State method,[13] in which the fluids are flowed simultaneously until steady-state equilibrium is established.

Gas permeability measurement by the stationary-phase method was relatively straightforward on both the drainage and imbibition cycles. This method also proved to be suitable for the measurement of water permeabilities on the imbibition cycle, but we were unable to obtain permeabilities to water under drainage conditions. Once a water saturation has been achieved by desaturation prior to testing, it always increased when water was introduced because the system was not kept under capillary control. The validity of the Penn State method is largely established on the imbibition cycle[14] and the use of unsteady-state techniques was precluded by the small pore volumes of the samples. Accordingly, the drainage water permeabilities were computed from their corresponding drainage gas permeabilities by the method of Corey.[14-15] Although this correlation is in wide usage in the petroleum industry, its applicability to highly fractured systems such as coal is tenuous.

All stationary-phase flow tests were performed with the apparatus described above. For the tests run by the Penn State method, the water was injected at constant flow rate by means of a high precision, positive displacement pump. All waters used in these tests were distilled and bacteria control was achieved via an in-line Millipore filter. All saturations were obtained gravimetrically.

Although slight variations in saturation (particularly during water permeability tests on the imbibition cycle) were evident prior to and after testing, the permeabilities were computed from Darcy's law and related to the average saturations. Such license is justified by the small saturation changes involved and by the work of Loomis and Crowell,[15] which shows that Darcy's law is a valid description of unsteady-state flows in gas-liquid systems at average saturation.

SATURATION PROCEDURES

Drainage Cycle

After the cores were prepared by the methods described above, the samples were initially evacuated and then completely saturated with water. Subsequently, the cores were desaturated by (a) blotting with an absorbent paper, (b) evaporation to the atmosphere, (c) exposure to flowing air at low pressure gradients and (d) partial evacuation at ambient temperature. Procedures a and b were employed at high water saturations, while procedures c and d were used at lower water saturations.

Liquid-Water Imbibition

The water saturation of the dried cores was increased by immersing the samples in distilled water for varying periods of time. These periods were initially of short duration because of the rapid imbibition of water by coal (indicative of a strongly water-wet medium).

Water-Vapor Imbibition

The dried samples were initially allowed to take up moisture from the atmosphere and later at higher saturations from the vapor phase of a desiccator saturated with water vapor.

Overburden Pressure

Overburden pressures were simulated by the confining pressures of the Hassler-type core holder. Geertsma[8] has shown that the pore compressibility of oil sands in a reservoir is about half of that measured under axially applied pressures. For a highly fractured structure such as coal, this observation would seem to be conservative. The overburden pressure, P_{ov}, was estimated from the confining pressure, P_{axial}, and the pressure gradient as

$$P_{ov} \approx 2(P_{axial} - \frac{\Delta p}{2}) \approx 2\ P_{axial} - \Delta p. \qquad (1)$$

For simplicity, the permeability curves are identified according to $P_{ov} = 2\ P_{axial}$, although the point values of P_{ov} were dependent on the actual variations in pressure gradient.

The stress hysteresis inherent in coal required that all runs be made at a single overburden pressure prior to their continuation at the next highest pressure.

GENERAL CHARACTERISTICS OF THE GAS RELATIVE PERMEABILITY CURVES

Figures 12 and 13 show drainage and imbibition gas relative permeability curves for four Pittsburgh and three Pocahontas samples. (Saturation distributions were obtained by liquid-water imbibition only). These were run at 400 psig overburden pressure by the stationary-phase method. The dashed curves represent generalizations of the actual data. Some general characteristics follow.

During drainage, the permeability to gas increases sharply for relatively small decreases in water saturation. This is followed by a plateau of almost constant permeability that is very close to the maximum value, K_a.

The imbibition gas relative permeability curves are in marked contrast to those for drainage. They may be roughly described as mirror images of the latter. In all cases, k_{rg} (imbibition) < k_{rg} (drainage), an observation common to oil cores. The gas permeability decreases rapidly with moderate water imbibition with some leveling off at higher water saturations. This behavior is a particularly true description of the Pittsburgh coal curves, but differs for those of Pocahontas inasmuch as for these samples there is only minimal change in the rate of permeability reduction throughout the saturation range.

The highly fractured structure of Pocahontas coal samples coupled with their severe permeability changes would seem to indicate that much of the flow is through large fractures.

The more gradual (although still severe) permeability gradients of the Pittsburgh coal are indicative of pore-size distributions of wider ranges. Indeed the greater reduction in nonwetting phases (air) permeability during imbibition vis-a-vis drainage as evidenced in Pittsburgh coal would seem to confirm this view as such behavior is usually associated with capillaric trapping.

These results appear to demonstrate the technical feasibility of water-infusion techniques as a means of controlling and abating the flow of dangerous gases (e.g., methane) from coal mines.

Characteristics of the Water-Vapor Imbibition Gas Permeabilities

The hysteresis of the imbibition and drainage gas permeability curves was more closely investigated for several samples. Drainage and liquid-water imbibition curves were obtained; then the dried samples were allowed to imbibe (or adsorb) water from the vapor phase as described earlier. The results were essentially identical for both samples and are illustrated in Figure 14 for Sample P-29. The solid curves are the drainage and liquid-water imbibition gas permeabilities that were obtained initially. The dashed curves represent a rerun of the tests with the imbibition curve being saturated from water vapor.

The striking similarity between the vapor-phase imbibition behavior and that of the drainage curves may be explained as follows. The moisture taken up by the dry coal samples is adsorbed onto the internal surface and enters a bound state. It is generally agreed[11] that the submicroscopic pores of coal in contact with saturated vapor become filled with adsorbed moisture, the properties of which differ greatly from those of normal water. Our findings indicate that this moisture content of coal does not interfere with the flow of gas up to relatively high water saturations (e.g., 80 percent). Such moisture content does, however, add weight to the sample and is accordingly reflected in the saturation determinations. Thus, the vapor-phase imbibition curve of Figure 14 is shifted in the direction of higher water saturation.

Gas and Water Permeabilities from Simultaneous Two-Phase Flow Tests

The results of a series of two-phase flow tests on a Pittsburgh coal sample are presented in Figure 15. The solid curves are the permeabilities to gas and water for both phases flowing simultaneously. The dashed curves represent the permeabilities to gas and water when only one phase is flowing. All tests were performed on the imbibition cycle.

The results indicate that both gas and water permeabilities obtained when both phases are flowing simultaneously are lower than those measured when only one phase is flowing.

The Effect of Overburden Pressure on the Effective and Relative Permeabilities

Drainage gas permeabilities and imbibition gas and water permeabilities were measured at three overburden pressures (200, 600 and 1,000 psig) for six Pittsburgh and four Pocahontas cores. Space does not permit the presentation of all of the results obtained, but Figures 16 through 22 are representative of the general behavior observed.

Figure 16 shows the effect of overburden pressure on drainage and imbibition gas relative permeabilities of PGH-2-1, a low permeability (0.43 md at P_{ov} = 200 psig) Pittsburgh coal sample. The drainage curves display only slight variance, although the effective permeabilities were drastically reduced. Conversely, the imbibition curves show a relatively large spread and a definite pattern of reduction with increasing overburden pressure.

Figures 17 and 18 show similar behavior for a Pittsburgh sample of much higher permeability, 17.8 md at P_{ov} = 200 psig. Figure 17 shows the marked reduction in gas effective permeabilities with increased overburden pressure over nearly all of the saturation histories. From 200-psig to 1,000-psig overburden pressure, the permeabilities are reduced as much as sixfold. Figure 18 repeats the characteristics observed in Figure 16 for PGH-2-1. It should be

noted that all of the relative permeabilities are computed from their corresponding effective permeabilities and the absolute permeabilities measured at the same overburden pressures as the former.

Figure 19 shows the relative gas permeabilities obtained for a very permeable Pocahontas coal (275 md at P_{ov} = 200 psig) that underwent a 13-fold reduction in permeability at 680 psig. With the exception of the drainage curve at 1,000 psig, the relative permeability curves are almost identical. Although the effective gas permeabilities of Pocahontas samples followed essentially the same pattern as those of Pittsburgh coal, their corresponding gas relative permeabilities showed little similarity as regards the sensitivity to overburden pressure during imbibition.

Figure 20 shows the measured imbibition, water relative permeabilities and the drainage relative permeabilities to water computed from their corresponding drainage gas permeabilities by Corey's[14] technique. The sample is a Pittsburgh coal with a gas permeability of 39.1 md at 200 psig and a water permeability of 110 md at 200 psig. This phenomenon (namely, that the permeability of coals to water is sometimes greater than that to gas) has been observed previously and was observed for several samples in the present study. The computed drainage curves display only slight dependence on overburden pressure, but are continually decreasing with increasing pressure. Similarly, the measured imbibition curves show only slightly greater dependence on overburden pressure, but tend to increase with increasing overburden pressure.

In a similar fashion, Figures 21 and 22 show the water permeability behavior of a Pocahontas core with a gas permeability of 34.6 md at 200 psig and a water permeability of 14.8 md at 200 psig. Although the effective permeabilities to water during imbibition are drastically reduced with increasing overburden pressure, the corresponding relative permeabilities display little spread. Again, the functional relationship between relative permeability and overburden pressure during drainage is opposite to that for imbibition. In most cases the permeabilities to water are higher during imbibition than during drainage, although the differences are less pronounced than those observed for gas. This result agrees well with many such observations noted for oil cores.[16]

Finally, we note that our method of measuring the water saturations is not completely satisfactory. To be accurate, the water content of a sample at a given overburden pressure should be associated with a pore volume measured at the same pressure. Values of the latter can only be obtained in a capillary pressure cell that permits the application of a confining pressure. Such a cell was constructed for the purpose of obtaining compressibility and capillary pressure data as functions of overburden pressure.

PART III, CAPILLARY PRESSURE STUDIES ON COAL SAMPLES

Various studies on the pore characteristics of Pittsburgh and Pocahontas coal were carried out. Many of these studies were performed to understand and overcome saturation problems connected with the permeability and relative permeability studies described earlier in this report. In addition, the effect of overburden pressure on the pore volume and the capillary pressure relationships was determined for a few samples.

Porosity Measurements

The porosity was determined by using both gas and water as the saturating fluid. Gas porosities of the coal samples were measured with a helium porosimeter. In determining the porosity of coal by the water saturation technique, dried and evacuated samples were allowed to imbibe water for a sufficient length of time (usually 48 hours as described earlier). The samples used in porosity measurements were not encapsuled and needed not be of uniform shape.

Pore Compressibility

The change in porosity with increasing overburden pressure was studied by measuring the pore compressibility for a number of samples from the Pittsburgh and Pocahontas coals. The 100 percent water saturated samples were placed in a triaxial, stainless steel Hassler-type core holder capable of handling pressures up to 10,000 psig. The Hassler sleeve was pressurized hydraulically with a hand pump. In a triaxial core holder the sample is subjected to an external stress field which is spherically isotropic. This simulates more closely the actual conditions in the coal seam and the overburden pressure will be equal to the applied confining pressure of the sleeve.

Changes in the pore volume of the samples were determined by measuring the incremental volumes of fluid displaced in a precision micropipette. A drop of red oil was added at the top of the fluid column to prevent evaporation of the displaced water.

Capillary Pressure Measurements

Two different types of capillary pressures measurements were made: (a) at atmospheric conditions and (b) at simulated overburden pressures up to 1,000 psig.

Two techniques have been widely employed in the petroleum industry for the determination of capillary pressures in porous media: the restored-state technique and the mercury injection technique.[18,19] The first method consists of placing a sample saturated with the wetting fluid on a semi-permeable plate or diaphram which is presaturated with the wetting fluid. The application of a given pressure on the non-wetting phase (usually gas) which is confined in a cell above the semi-permeable plate results in the expulsion of a portion of the wetting phase through the plate. In the mercury injection method, mercury (a non-wetting phase to most rocks) is injected under pressure into the sample. The mercury vapor and the residual gas correspond to the wetting phase.[18]

While the mercury injection method is considerably faster, the restored state technique has the advantage of being capable of employing the actual fluids of interest and not contaminating the samples as does the mercury injection.

Capillary pressure curves for coal at zero confining pressure (atmospheric) were obtained in a standard Ruska cell using the restored-state technique. The coal samples were 100% saturated with water and were not encapsuled or mounted in sleeves. Air was used as the displacing phase.

Capillary Pressure Measurements at High Confining Pressures

The apparatus shown in Figure 23 was set up for measuring capillary pressures at high confining pressures. External pressures were exerted on the sample in a Hassler core holder. A semi-permeable porcelain plate with a bubbling pressure of 80 psig was fitted to the outlet face of the end-plug of the core holder. This converted the core holder to a capillary pressure cell inasmuch as it acts as a barrier to the passage of air when saturated with water. The principle drawback was the constraint of unidirectional macroscopic displacement. However, Brown[19] has shown in his "dynamic capillary-pressure" technique that unidirectional displacement yields almost identical results to those obtained by the multi-directional displacement of the restored state and mercury injection methods.

The water displaced from the sample was collected and measured in an inverted micropipette.

RESULTS AND DISCUSSION OF THE STUDIES ON PORE CHARACTERISTICS

Helium and Water Porosities

In any water-gas relative permeability study one must be able to express the water and gas saturations at each value of the water and gas permeabilities. Therefore the porosity of coal was determined by using both water and gas as the saturating fluid. As expected, the results were somewhat different when using the two different fluids.

Table 8 lists the results of saturation determinations for several samples from the Pittsburgh coal. It can be seen that the porosity as determined by helium is much higher than the value obtained by saturating the samples with water. The helium porosity values ranged from 2.6% to 8.6% but the values calculated from water saturations varied from a low of 0.4% up to 1.1%. These results agree well with observations by Von Krevlin and Schuyer[20] who point out that most coals have

different sets of pore systems. All of the pores are accessible to helium but only the larger pores (the fractures or cracks) are accessible to liquids such as water or mercury, even if the latter is under high pressure. The implication of this fact is that the point of 100% water saturation may not mean that the gas saturation is not zero even though no more water can enter the coal. It must be recognized however that not all the pores penetrated by helium are accessible to other gaseous molecules such as air or methane and the values of the water and air porosities may not be so far apart.

Because small quantities of water are involved in saturating the coal samples (often about 0.1 to 1.0 gr.) a very small amount of water clinging to the outer surface of the sample could have a large effect on the porosity. Therefore the precision of the method was checked by subjecting some samples to repeated immersions. The results showed that the wet weight varied only in the milligram range. When converted to porosity, this variation changes the porosity by only 0.01 to 0.02%. Therefore it was assumed that the method should provide good values for the porosity of coal as determined by water saturation.

Variables Affecting the Measured Porosity

It was pointed out earlier that significant variations in the porosity of coal as measured by water saturation are caused by changing the length of time that each sample is allowed to soak in water.

It also appeared that the porosity of coal samples increased if samples are dried in a vacuum oven at 90°C. Table 9 shows that the porosity as measured by helium increased for each sample, the largest increase being about 38%. The porosity as determined by water increased by a large relative amount in each case; in sample B-1 the porosity, as measured by water, more than doubled when the sample was dried in an oven. These observations demonstrate the existance of both "free" and "bound" moisture in the coal.

The porosity of coal was found to be sensitive to the overburden pressure. This effect is discussed in the following section. Table 10 lists the porosity and permeability of some Pittsburgh and Pocahontas coal samples at various overburden pressures. It is evident that the porosity at any pressure is always less than the porosity of the sample at atmospheric conditions.

Pore Compressibility

In this series of tests the coal samples were subjected to the same overburden pressure along the three principle directions in the triaxial core holder. The porosity at atmospheric pressure, $\Phi(P_{ov})$, was computed assuming that the bulk volume remains constant. This assumption is very reasonable because of the much larger solid volume compared to the pore volume (porosity of coal is generally less than 5%) and also very small solid compressibility as compared to the pore compressibility.

Figures 24 and 25 are plots of Φ vs P_{ov} for four samples from the Pittsburgh and five Pocahontas coal samples. It is evident that Φ decreases with increasing P_{ov}. The rate of decrease of porosity with pressure is greater for the Pocahontas coal and is more significant for both coals at overburden pressures below 1500 psig. The pore compressibility $\frac{d\Phi}{dP}$ becomes almost constant at pressures greater than 1000 psig.

Atmospheric Capillary Pressure Curves

Drainage capillary pressure curves were obtained for a number of Pittsburgh and Pocahontas coal samples in a standard Ruska cell. Most of the samples were 1½-in. diameter cylindrical core plugs. The pore volume was calculated from the amount of water imbibed by the dried and evacuated coal samples over a period of 48 hours. Displacement pressures ranged from as low as 3.5 cms. of red oil to 75 cms. of mercury (equivalent P_c range (7.4×10^3 to 2.54×10^6 dynes/cm^2)). At each displacement pressure several readings of the volume of the displaced fluid were taken until near equilibrium conditions were attained.

Figure 26 is an example plot of the capillary pressure curve for a Pittsburgh coal sample. The "irreducible" or minimum water saturation for oven dried coal samples was found to be approximately 45%. However, for air dried samples the minimum water saturation varied between 25% and 75%. Previous studies of the nature of water in coal indicated that the total moisture content of a given type of coal is constant while the air dried moisture (free or unbound water) depends on a number of variables.[11]

Not all samples displayed a uniform curve as that shown in Figure 26. Many samples produced skewed or discontunuous curves depending on the makeup of the pore space of a fracture network and/or a system of pores of varying sizes. Plateaus in the P_c curves corresponded to the desaturation of flow channels or a crack of a fairly uniform size.

Effect of Overburden Pressure on the Capillary Pressure Curves

The capillary pressure curves obtained in the Ruska cell are at a confining pressure of zero. To study the effect of higher overburden pressures on the capillary pressure curves, pore structure and size distribution the apparatus of Figure 23 was used.

Compressibility studies have shown that the porosity of coal samples decreases with increasing overburden pressure. This change in pore volume with overburden pressure was found to be more significant in the range 0-1000 psig. For this reason the water saturations at any overburden pressure were based on the available pore volume at that particular pressure.

Figure 27 is a plot of the capillary pressure curves for a coal sample at three different overburden pressures: P_{ov} = 200, 600 and 1000 psig. The results clearly showed a marked dependence of the capillary pressure distributions on the overburden pressure. Figure 27 indicates the relationship to be the result of a simple dilatational deformation where the curves undergo fairly uniform shifts towards increasing displacement pressures and water saturations (smaller pore sizes) as P_{ov} increased. More complex changes in capillary pressure distribution with variation in P_{ov} are illustrated in Figure 28. Such complex changes might result from more complex deformations such as rotational, angular and dilatational. Therefore, as some pore channels decrease in size others may increase. Also, our studies of the effect of overburden pressure on the permeability of coal to air and water indicated that repeated application and release of external stress on coal samples can result in altering the flow characteristics of the samples entirely.

Pore Size Distribution

Equivalent pore sizes were calculated from the capillary pressure data from the relationship

$$r = \frac{2\sigma \cos \theta}{P_c}$$

The interfacial tension σ between air and water is about 72 dynes/cm and assuming that water completely wets coal, cos θ is equal to one. Hence,

$$r(\text{microns}) = \frac{1.44 \times 10^6}{P_c \ (\text{dynes/cm}^2)}$$

It is recognized that the contact angle θ has been measured on a number of samples and it normally is somewhat greater than zero. However, in our tests it is clear that we are dealing with receding contact angles and these are usually small. Values ranging from 18° to 38° appear in the Literature.[21] Since cos 20° is 0.94, the use of 1.0 (from the assumption of zero contact angle is justified in preliminary calculations for the sake of simplicity.

Figure 29 is a plot of the equivalent pore radius r vs f_i, where f_i is the fraction of pore volume comprised of pores of radii $\geq$ r for a collection of Pittsburgh coal samples at atmospheric pressure. The complexity of the pore structure of coal being comprised of systems of pores and fracture networks was clearly demonstrated by the size distributions. Plateaus in the curves correspond to cracks or fracture of a given size and vertical portions correspond to discontinuities in the pore size distribution.

The range of pore sizes determined for coal at atmospheric conditions (no external stress) was found to be from 0.1 to 200 microns. Interestingly, these pore sizes calculated for coal from drainage gas-liquid capillary pressure data are within the range found for other types of coal in a previous study of the porosity of coal by the mercury injection method.[9]

Effect of overburden pressure on the pore size distribution is evident from the results of Figure 30. These size distributions at three different overburden pressures are for the same sample for which the corresponding P_c curves are presented in Figure 27. In this case a uniform shift in the direction of decreasing equivalent pore sizes was obtained as the overburden pressure increased. However, as mentioned earlier many samples displayed a much more complex behavior and such uniform shift with increasing P_{ov} was not always obtained.

DISCUSSION AND POSSIBLE APPLICATIONS OF THE PERMEABILITY AND RELATIVE PERMEABILITY RESULTS

Methods which have been attempted for controlling dangerous gases in mines include the drainage of methane through boreholes or water infusion. Water infusion also has considerable importance in the mining industry as a means of reducing airborne dust. In each case, the effectiveness of these measures is dependent to a great extent on the permeability of the coal to gas or water and on the prevailing pressure gradients.

As to the gas permeability, the results of the present study on the Pittsburgh and Pocahontas coals indicated a wide variation in the permeability of samples from the same coal and even from the same coal chunk. All coals, particularly the friable ones like the Pocahontas, are full of cracks, fissures or cleats ranging in size from those that can be seen with the naked eye to those that are microscopic or even submicroscopic. The permeability of a sample thus depends on how many cracks of any given size are present in that sample. It has been shown that solid unfractured coal is virtually impermeable and that fractures are present wherever a flow of gas can be detected.

While previous studies[2,3] on other types of coal stopped at defining a range for the gas permeability of a given coal, we believe a permeability distribution similar to that in Figure 4 is a more definite characterization.

It must be emphasized that it is difficult to be unequivocal about the absolute permeability of a specific coal sample to gas because the observed permeability varies with the confining pressure, which may be compared with the overburden pressure, and with the mean flow pressure.

Overburden has the most significant effect on gas permeability. The permeabilities of all of the Pittsburgh and Pocahontas coal samples decreased markedly when the simulated overburden pressure on the sample was increased. The strong hysteretic behavior displayed by all samples

shows that the stress history is also critical. It is concluded that under the application of external mechanical stress coals exhibit a plastic-elastic deformation behavior that affects their flow characteristics in a very significant fashion.

Reduction in permeability with increasing mean flow pressure was less significant. At P_∞, the gas permeability is reduced by about 10-20% for most of the samples, although a reduction in permeability as high as 66.7% was observed for a low permeability samples. The unusual Klinkenberg behavior displayed by low permeability samples at subatmospheric mean flow pressures deserved some attention. Two factors might have contributed jointly or separately to the rapid increase in the gas permeability in the range, $1 < 1/P_m < 2$. In low permeability sections of the coal the presence of large fractures is highly unlikely and the flow of gas takes place in microscopic and submicroscopic pore spaces, some of which are of molecular size. It has also been established that the gaseous constituents of air, oxygen nitrogen and carbon dioxide, are adsorbed to various extents on the internal surface of coal. It was found that this adsorption process causes swelling at the adsorption sites and subsequent blockage of adjacent pores.[9] It appears that at subatmospheric pressures a desorption process starts, thus opening new channels for gas molecules to flow and adding the desorped molecules to the total flow. Once all or most of the blocked channels have been opened, the rate of increase in permeability with further decreasing pressure becomes considerably smaller as indicated by Figure 5.

It is also evident that moisture is more strongly adsorbed on the internal surface of coal as compared with the gaseous molecules of air. This explains why there was no appreciable increase in permeability with decreasing P_m along the second line segment when the sample contained 1.3 percent by weight moisture (Figure 5).

Studies of the effect of the presence of water saturation on the permeability to gas of various oil reservoir rocks indicated that the Klinkenberg effect is reduced as the water saturation in the core sample increased.[10] Figure 5 shows that the presence of moisture in coal causes a similar effect.

We believe this area needs further investigation, although such an investigation may appear to be academic.

Infusion of water in coal will be controlled by the water permeability of the coal and the pressure gradients. The results of this work indicated that gas and water permeabilities of coal samples could be quite different. Theoretically, the single-phase gas permeability of a porous rock sample, when extrapolated to $1/P_m = 0$, K_∞, should be equal to its permeability to a nonreactive liquid completely saturating the sample. There are reasons to presume that such a conclusion may not be true for the case of flow of water in coal. The water-coal system is not totally nonreactive as compared with an oil-sandstone situation. For instance, water is strongly adsorbed in the submicroscopic pores of coal and the properties of the adsorbed moisture differ greatly from those of normal water.[11] The amount of moisture adsorbed by coal varies with external conditions such as humidity of the atmosphere, temperature, etc. It is also known that expansion accompanies the uptake of water by coal that results in a reduction of the effective area available to flow or the blockage of some flow channels.[24]

In general, if the flowing water pressure is much smaller than the overburden pressure, the permeability of coal to water is smaller than the gas permeability. However, it is possible for the water permeability to be greater than the gas permeability, particularly if high pressure gradients are applied. This is due to the tendency of the high pressure flowing water to induce mechanical fatigue of the coal that results in the opening of fractures and cleats. In fact, hydraulic fracturing of coal has been practiced in the field recently, and experience has shown that large volumes of water can be injected directly into the coal seam as long as high injection pressures are used.

The water-gas relative permeability results can be useful in explaining aspects of methane evolution and possible control techniques that may be applied in coal mines. All of the results indicate that the gas permeability rises rapidly as water is removed from the coal. On the drainage cycle the gas permeability normally reaches 100 percent before the water saturation drops to 50 percent. This large increase in gas permeability may explain the situation

wherein gas evolution is sustained at high values even after the natural methane pressure gradient has fallen over a period of many months.[17] In some of these cases the water drained continuously from the mine, thus permitting the relative permeability of the gas to increase while the pressure gradient was falling.

The imbibition relative permeability curves support the expectation that water-infusion techniques can decrease gas evolution into mines at the working face.[17] In most of the liquid-imbibition experiments the gas permeability dropped to less than 40 percent of the "dry coal" permeability when the coal had imbibed water equal to only 40 percent of pore volume. In the water-infusion method it is assumed that the water saturation is increased in a manner that would follow the liquid imbibition curve. Therefore, water injected into the coal seam should retard the flow of methane as long as the water saturation is increased to 40 percent or more of the pore volume of the coal.

SUMMARY AND CONCLUSIONS

1. Variations of more than four orders of magnitude can be expected for the single-phase (gas or water_ permeabilities of samples from the Pittsburgh and the Pocahontas coals.

2. Both air and water permeabilities are greatly reduced by increases in the overburden pressure. Both displayed significant hysteretic behavior.

3. Mean flow pressures above atmospheric have a small effect on the single-phase air permeability of both coals. However, at subatmospheric flow pressures, appreciable increases in the air permeability can be expected for tight sections of the coal with permeabilities below 10 md.

4. At high overburden pressures the water permeability is smaller than or equal to the air permeabilities. When the confining pressures are low (below 200 psig), the water permeability can exceed the air permeability due to

the tendency of the coal to fracture internally under the shear stresses of the flowing water.

5. Two-phase permeabilities for both the drainage and imbibition cycles have been obtained for Pittsburgh and Pocahontas coal.

6. Permeabilities to gas are substantially lower during imbibition than during drainage. Both cases reveal the feasibility of methane abatement in coal mines by water-infusion techniques.

7. The gas drainage curves are characterized by nearly constant and largely undiminished permeability values over much of the saturation range. The corresponding imbibition curves may be approximately described as mirror images of the drainage curves.

8. Water permeabilities are typically represented by steep curves and are higher on the imbibition than on the drainage cycle.

9. Gas permeabilities resulting from water-vapor imbibition differ radically from those measured for liquid-water imbibition. The latter is significantly lower than and the former almost coincident with the corresponding drainage curve. This behavior indicates that the adsorbed moisture exists largely in a bound state in micropores and does not interfere with flow.

10. Permeabilities to both phases are drastically reduced when subjected to increasing overburden pressure. However, relative permeabilities tend to be more closely spaced and are quite similar in shape, particularly for the drainage case.

NOMENCLATURE

K_a = permeability to air, millidarcy (md.)

K_{ai} = permeability to air at the lowest overburden pressure, md.

K_∞ = air permeability extrapolated to infinite mean flow pressure, md.

K_w = permeability to water, md.

k_{rg} = gas relative permeability

P_{axial} = confining (sleeve) pressure, psig.

P_c = capillary pressure, dynes/cm^2

P_m = mean pressure at center of coal sample, atm

P_{ov} = simulated overburden pressure, psig. ($P_{ov} \approx 2\ P_{axial}$)

P_{ovi} = initial (lowest) overburden pressure, psig.

r = pore size, microns

v = water flux, cc/cm^2-hr.

$\frac{\Delta p}{\Delta x}$ = pressure gradient, atm/cm.

θ = contact angle of water on coal, degrees

μ_w = water viscosity, centipoise (cp)

σ = surface tension of water, dynes/cm.

ϕ = porosity percent

REFERENCES

1. Cervik, J., "The Behavior of Coal-Gas Reservoirs," Paper SPE 1973 presented at the SPE Eastern Regional Meeting, Pittsburgh, Pa., Nov. 2-3, 1967.

2. Huang, W. M. and Shelton, C., "Experimental Results of Coal Permeability Tests," Trans., AIME-Mining (1962) 225, 245-247.

3. Patching, T. H., "Variations in Permeability of Coal," Proc., Rock Mechanics Symposium, Toronto (1965) 185-199.

4. Fish, B. H. and Turski, A. B., "The Flow of Water Through Coal," I. Colliery Eng. (Jan. 1957) 16-20 and II. Colliery Eng. (Feb. 1957) 55-58.

5. Evans, I. and Skinner, D., "The Permeability of Coking Coal to Water at Low Pressures," Colliery Eng. (Aug. 1960) 341-346.

6. Pomeroy, C. D. and Robinson, D. J., "The Effect of Applied Stresses on the Permeability of a Middle Rank Coal to Water," J. Rock Mech. Min. Sci. (1967) 4, 329-343.

7. Klinkenberg, L. J., "The Permeability of Porous Media to Liquids and Gases," Drill. and Prod. Prac., API (1941) 200-213.

8. Geertsma, J., "The Effect of Fluid Pressure Decline on Volumetric Changes of Porous Rocks," Trans., AIME (1957) 210, 331-340.

9. Zwietering, P. and Van Krevelen, D. W., "Chemical Structure and Properties of Coal., Part IV-Pore Structure," Fuel (1954) 33, 331-337.

10. Estes, K. R. and Fulton, P. F., "Gas Slippage and Permeability Measurements," Trans., AIME (1956) 207, 338-341.

11. Bond, R. L., Griffity, M. and Maggs, F. A., "Water in Coal," Fuel (1950) 29, 83-93.

12. Coal News, N.C.A., 3, (4132), Oct. 20, 1973 (current USBM project in Hanna, Wyo.).

13. Scheidegger, A. E., The Physics of Flow Through Porous Media, Macmillan Co., New York (1960) 218-224.

14. Corey, A. T., "The Interrelation Between Gas and Oil Relative Permeabilities," Prod. Monthly (1952) 19, No. 1, 38.

15. Loomis, A. G. and Crowell, D. C., "Relative Permeability Studies: Gas-Oil and Water-Oil Systems," Bull. 599, USBM (1962).

16. Reznik, A. A., Fulton, P. F. and Colbeck, S. C., "A Mathematical Imbibition Model with Fractional Wettability Characteristics," Prod. Monthly (1967) 31, No. 9, 22.

17. Kissell, Fred N., "Methane Migration and Storage Characteristics of the Pittsburgh, Pocahontas Number 3, and Oklahoma Hartshorn Coal Beds," RI 7667, USBM (1972).

18. Rose, W. and W. A. Bruce, "Evaluation of Capillary Character in Petroleum Reservoir Rock," Trans. AIME, 186 (1949), 127.

19. Brown, H. W., "Capillary Pressure Investigations," Trans. AIME, 192 (1951), 67.

20. Von Krevelin, D. W. and Schuyer, J., "Coal Science Aspects of Coal Constitution," Elsevier, New York, 1957.

21. Smith, H. and Duckmanton, B., "Further Contact Angle Studies at Coal Surfaces," Second Symposium on Coal, U. of Leeds, Oct. 21-23, 1957, Paper No. 15.

22. Lal, Sunil B., "The Measurement of Porosity by Using Helium, Water, and Mercury as the Saturants and Air Permeability of Coal," M.S. Thesis, University of Pittsburgh, School of Engineering, 1973.

23. Talaat, Ismail M., "Measurements of Flow Properties of Pocahontas and Greenwich Coals and Factors Affecting These Measurements," M.S. Thesis, University of Pittsburgh, School of Engineering, 1972.

24. Gregg, S. J., "The Surface Chemistry of Solids," Reinhold Publishing Corp., New York, 1961.

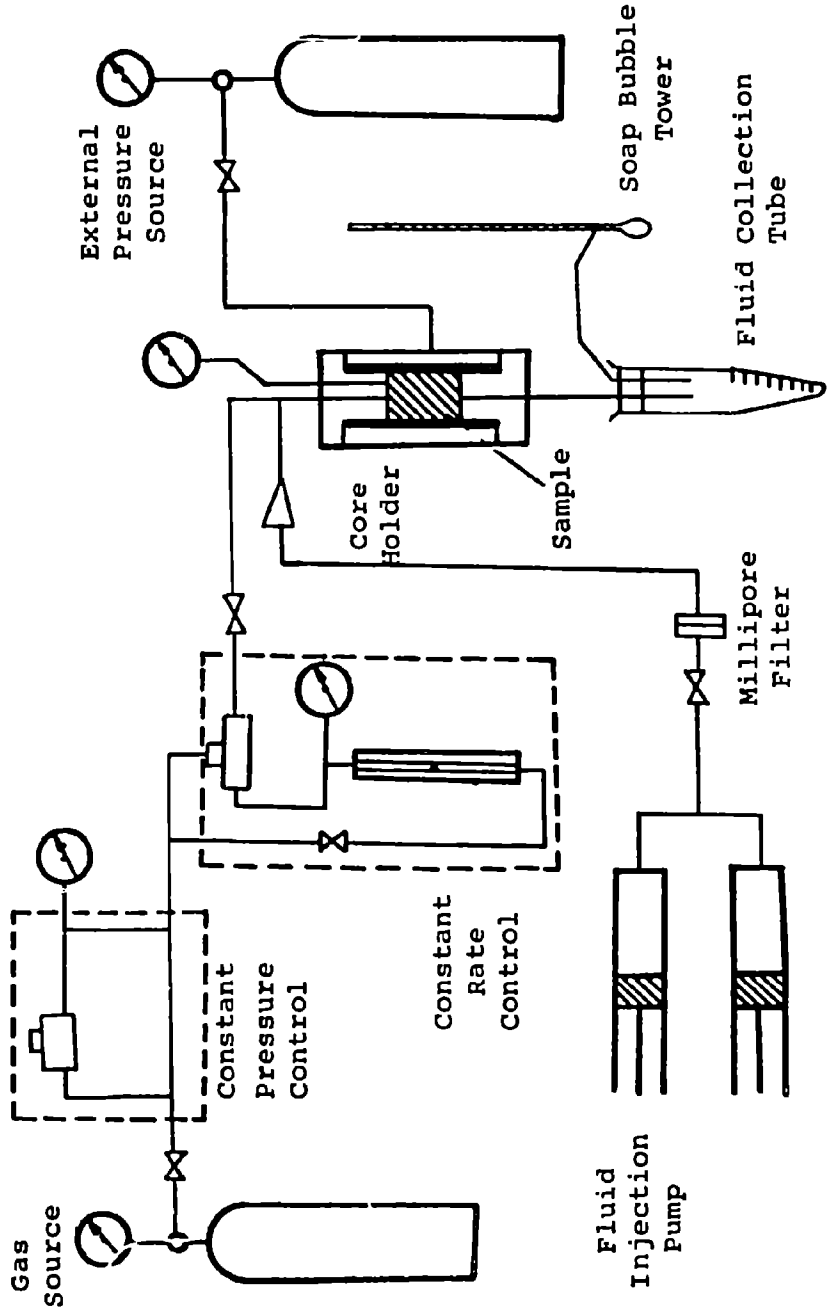

FIGURE 1: EXPERIMENTAL APPARATUS FOR MEASURING ABSOLUTE AND RELATIVE PERMEABILITIES.

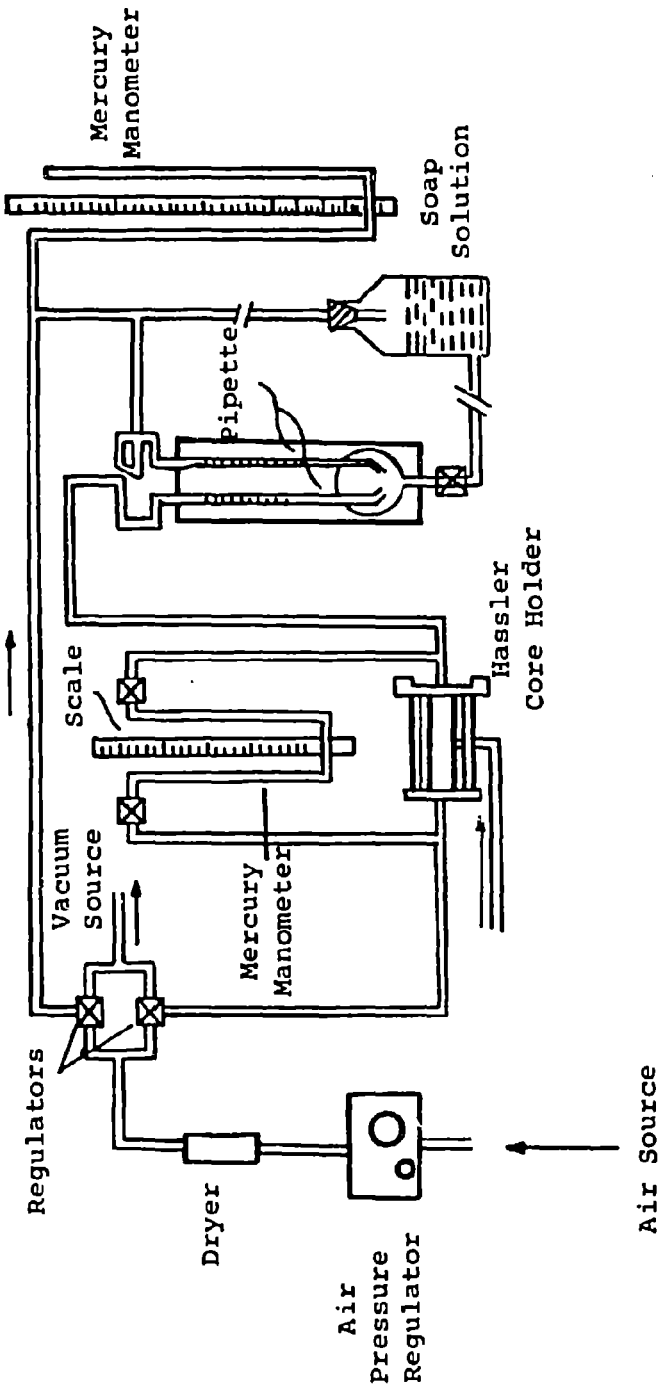

FIGURE 2: EXPANDED MEAN PRESSURE RANGE PERMEAMETER.

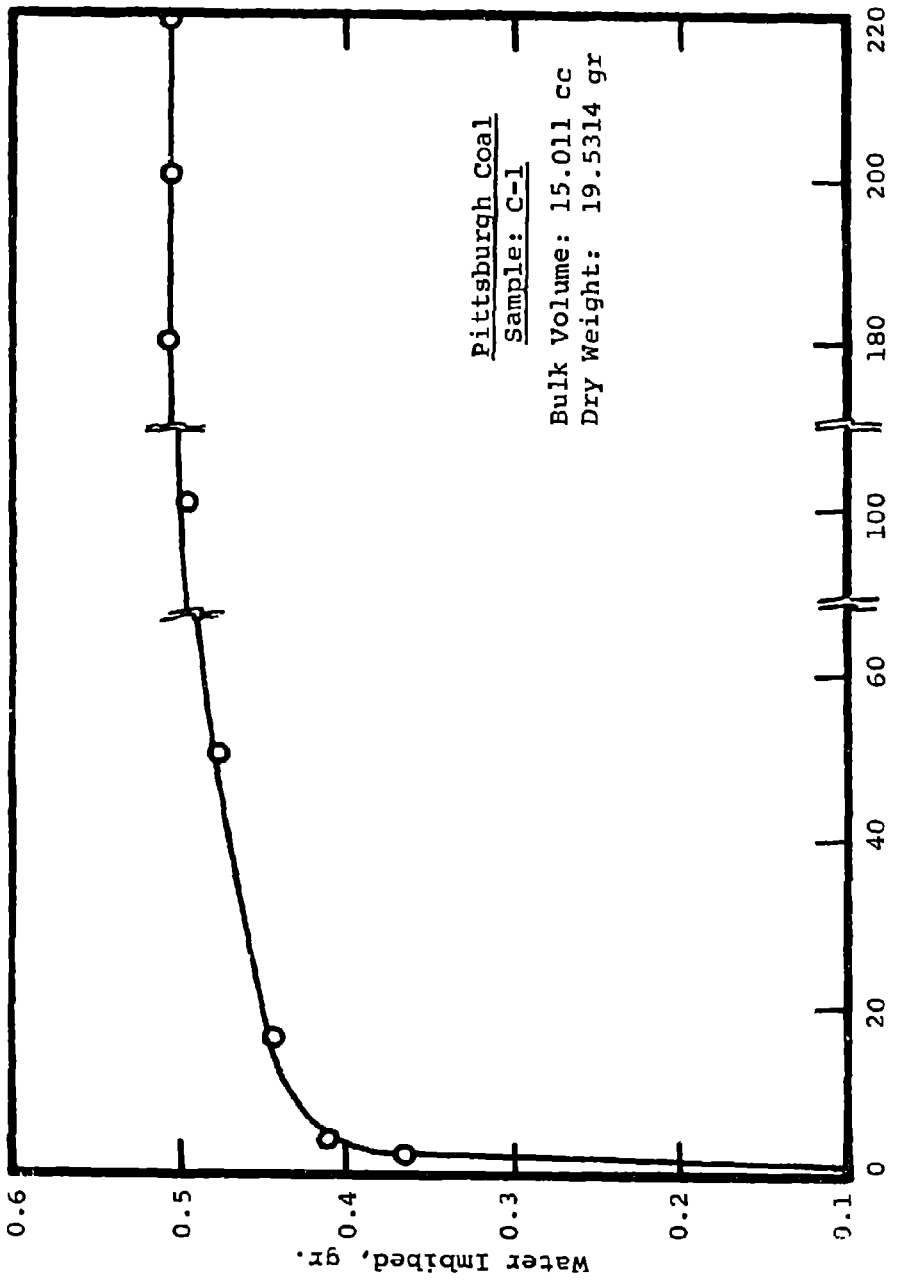

FIGURE 3: IMBIBITION OF WATER BY COAL.

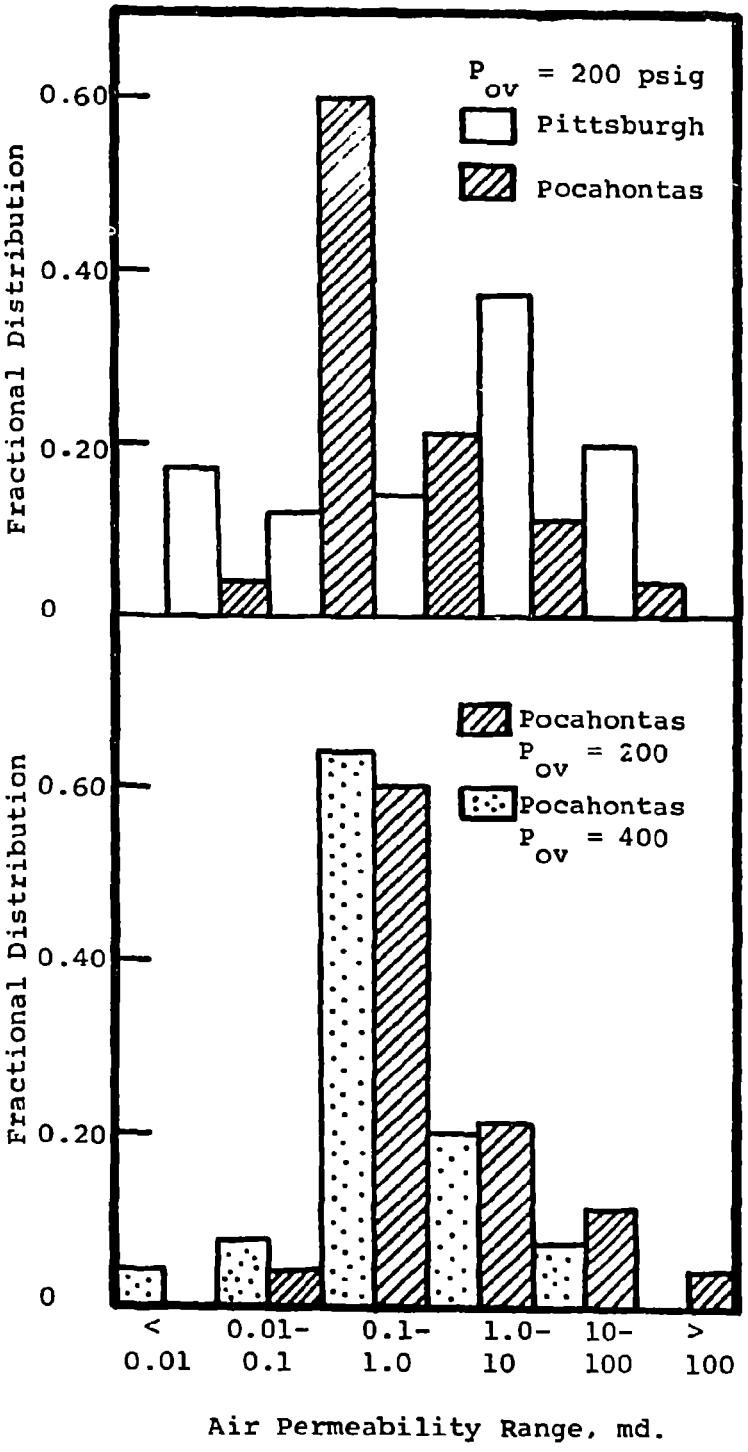

FIGURE 4: AIR PERMEABILITY DISTRIBUTIONS FOR PITTSBURGH AND POCAHONTAS COALS.

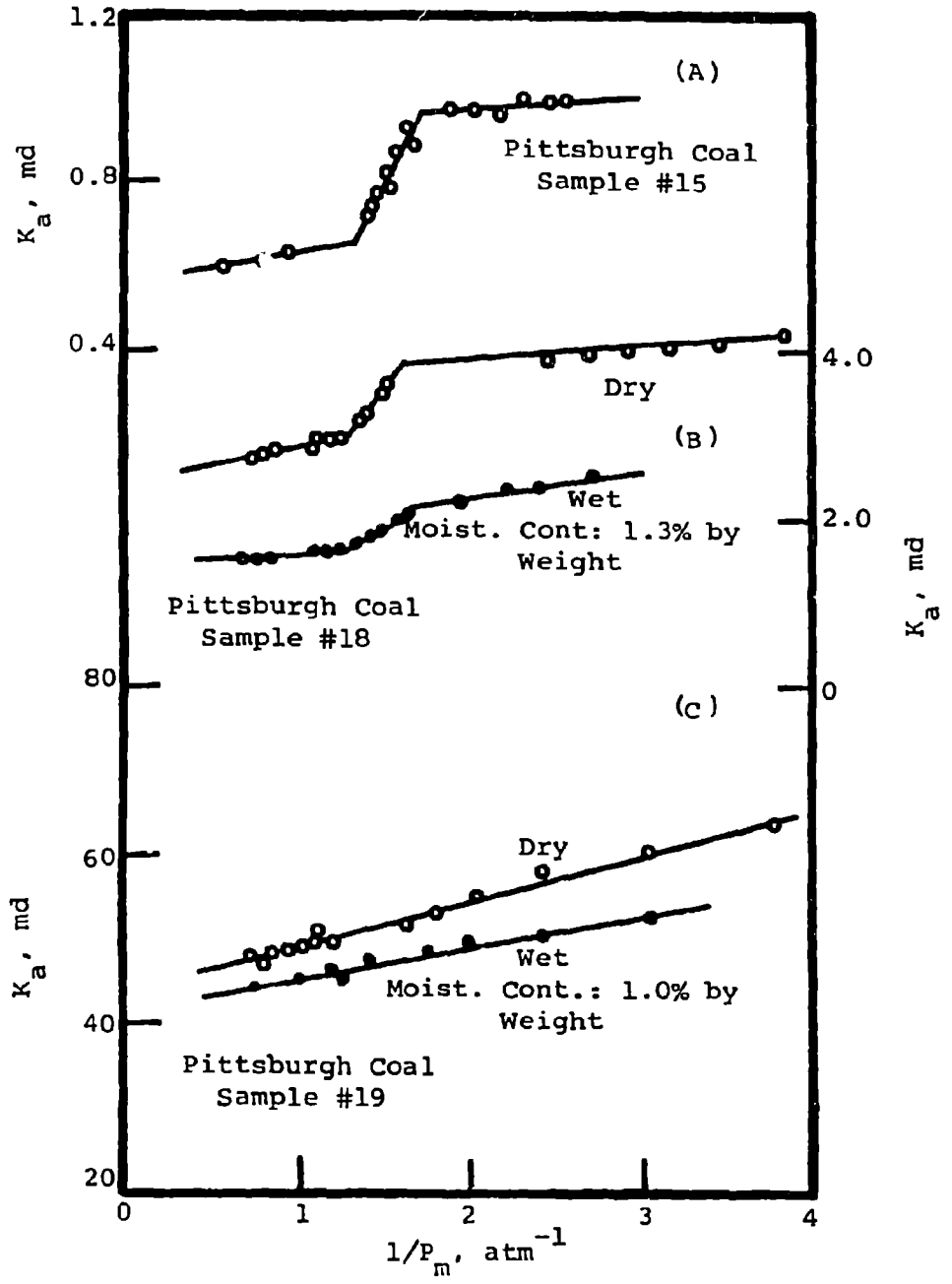

FIGURE 5: EFFECT OF MEAN FLOW PRESSURE ON THE AIR PERMEABILITY OF COAL.

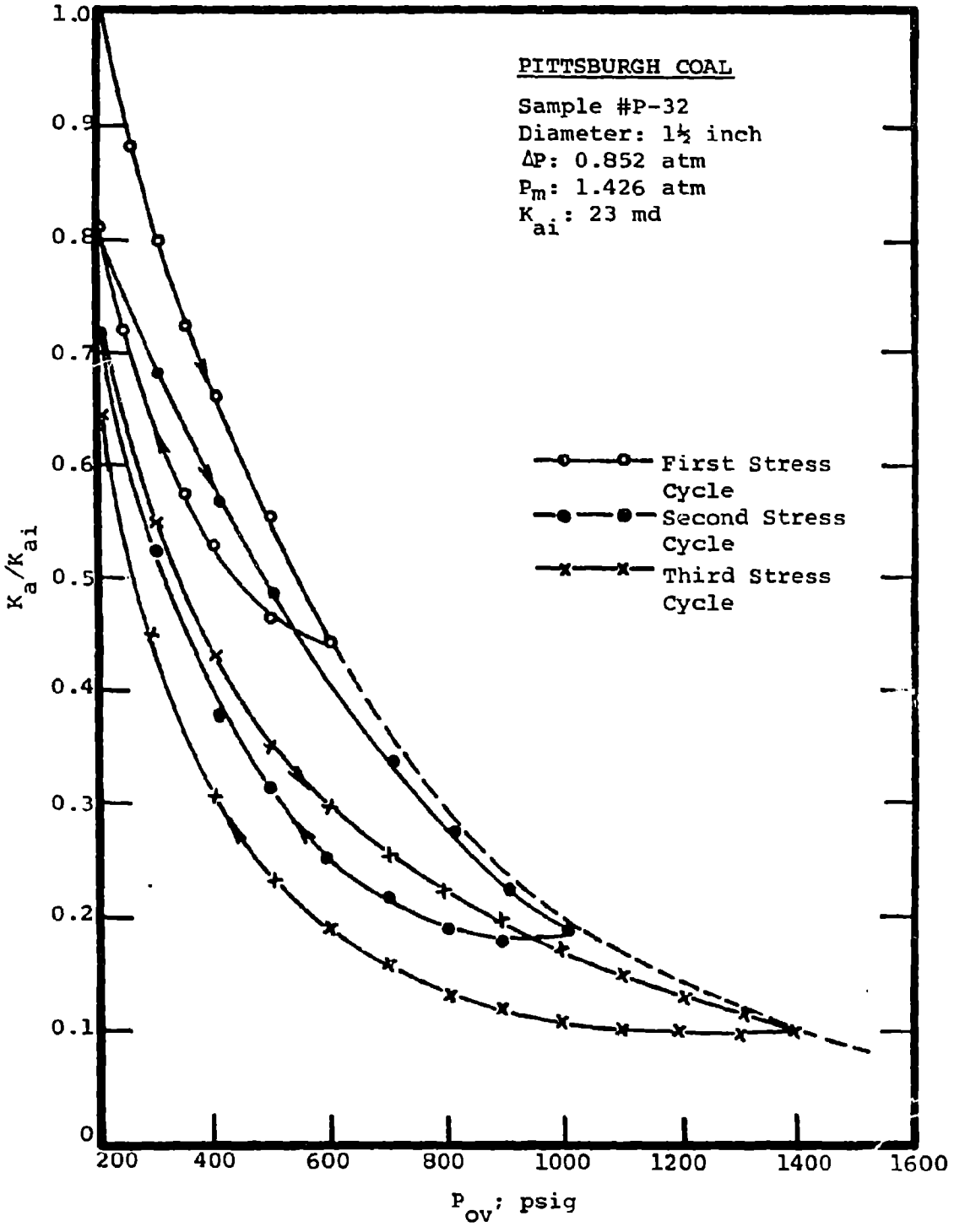

FIGURE 7: PERMEABILITY HYSTERESIS IN COAL, EFFECT OF OVERBURDEN PRESSURE.

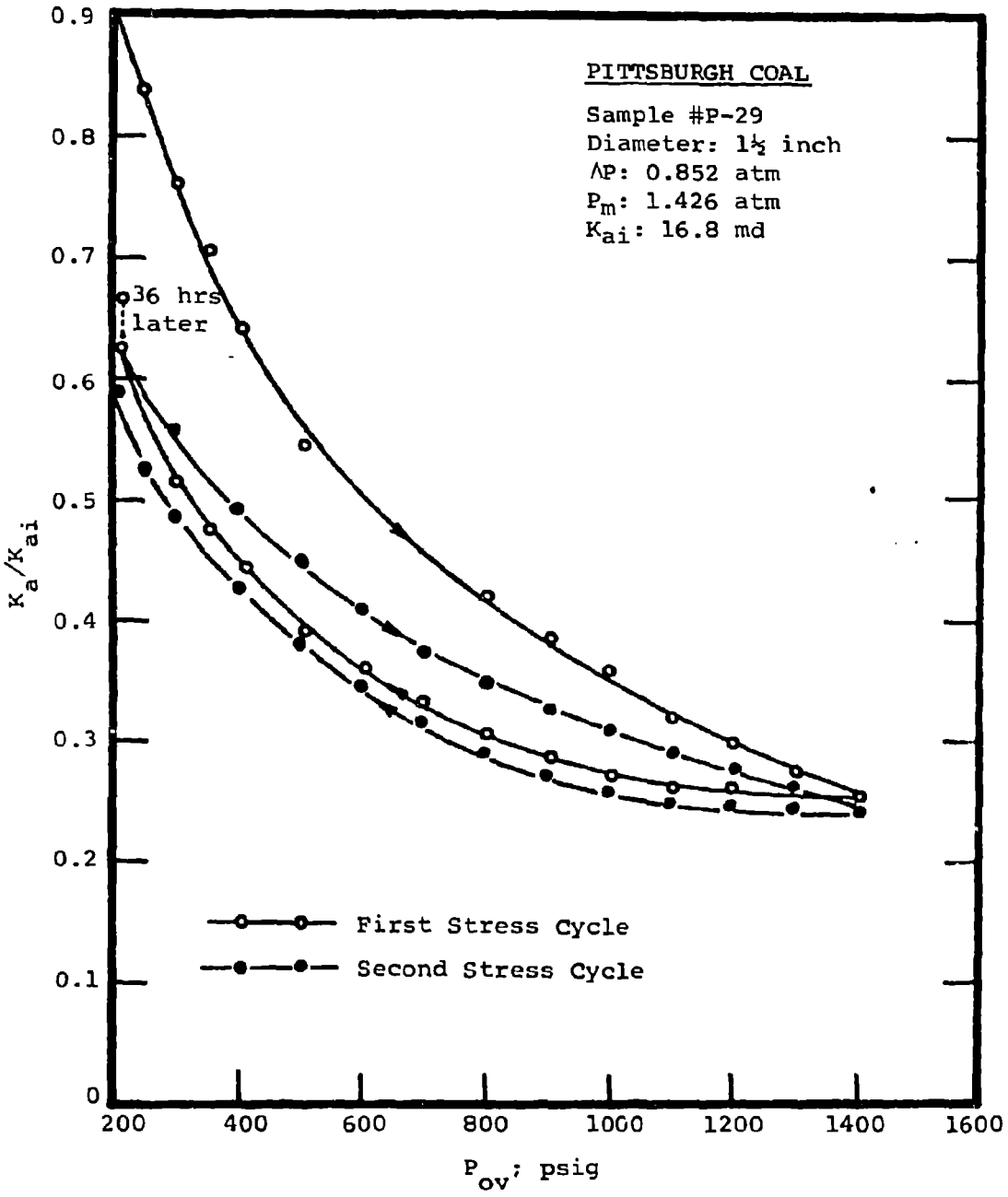

FIGURE 6: PERMEABILITY HYSTERESIS IN COAL, EFFECT OF OVERBURDEN PRESSURE.

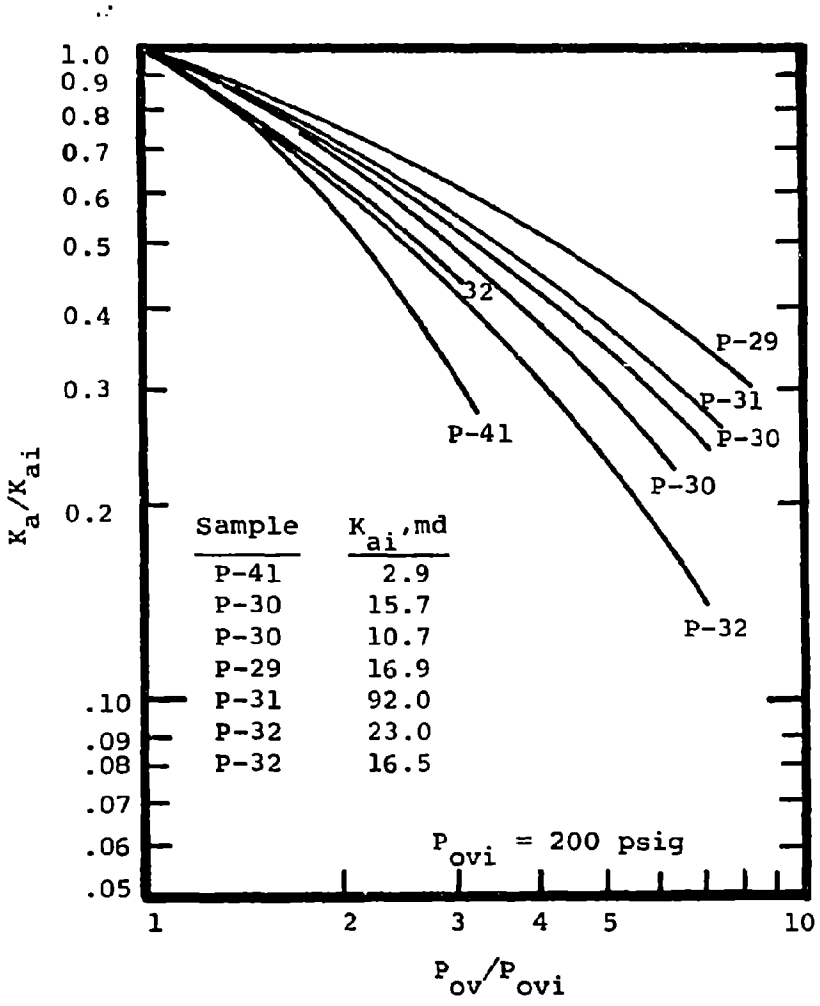

FIGURE 8: VARIATION IN PERMEABILITY WITH OVERBURDEN PRESSURE RATIO SAMPLES FROM THE PITTSBURGH COAL.

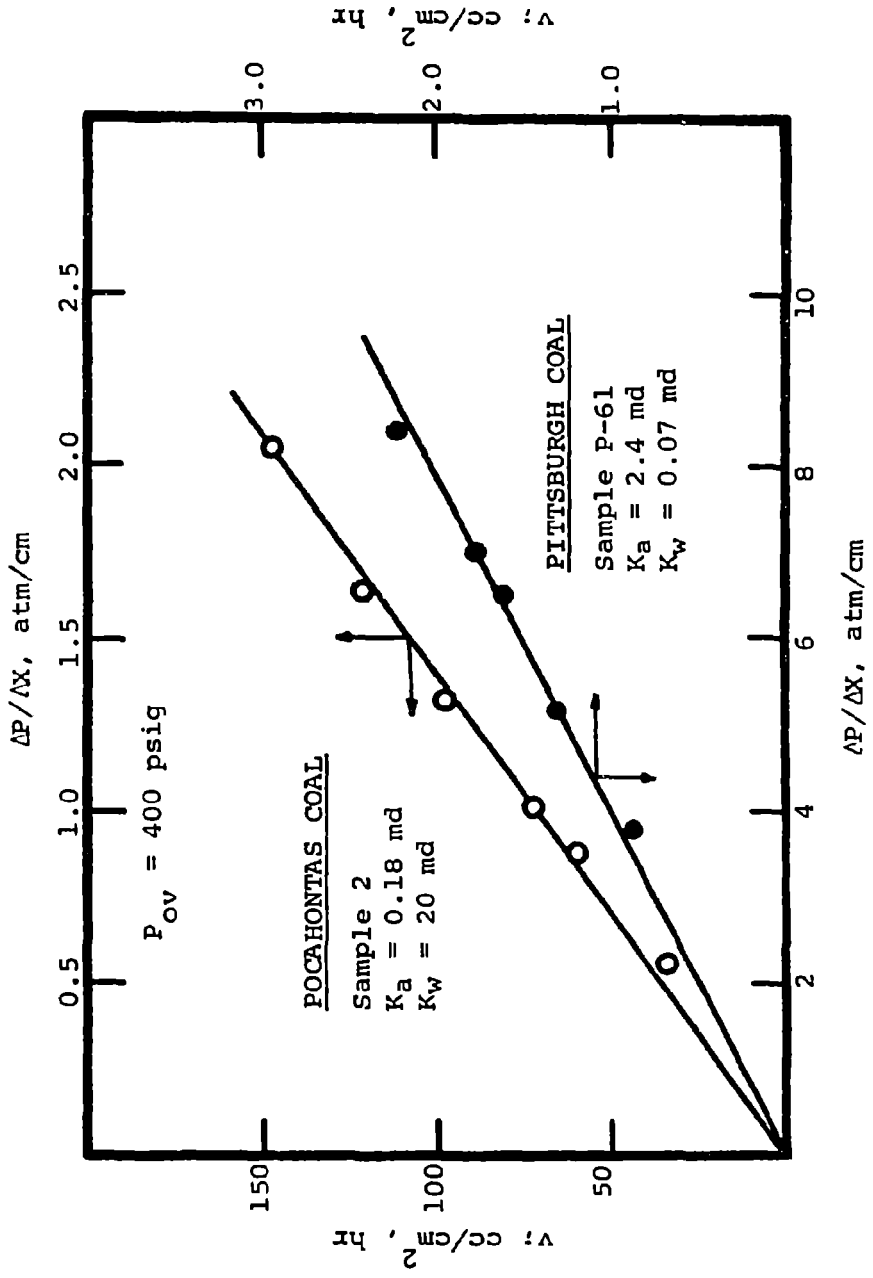

FIGURE 9: WATER FLUX, v, vs. PRESSURE GRADIENT, ΔP/ΔX; FOR 100% WATER SATURATED COAL SAMPLES.

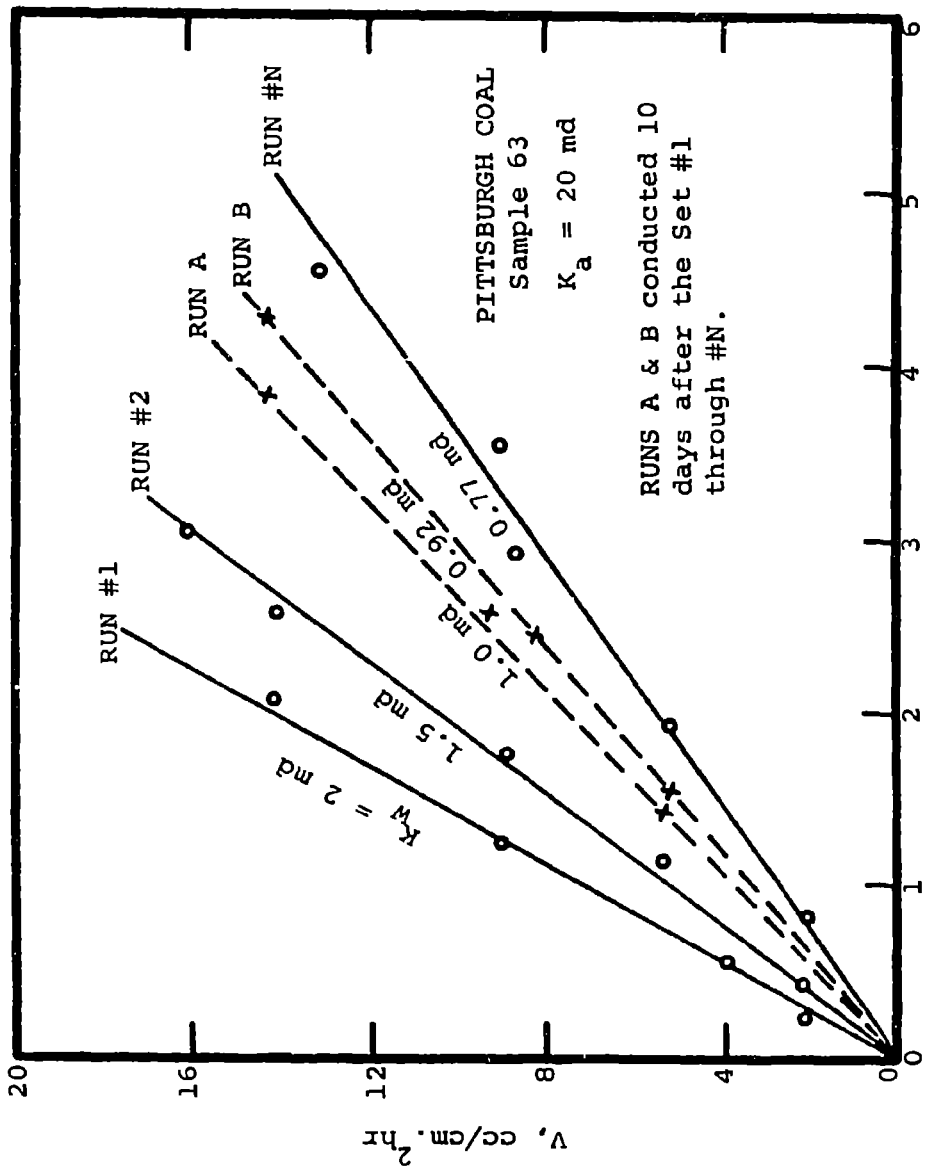

FIGURE 10: WATER PERMEABILITY HYSTERISIS IN COAL

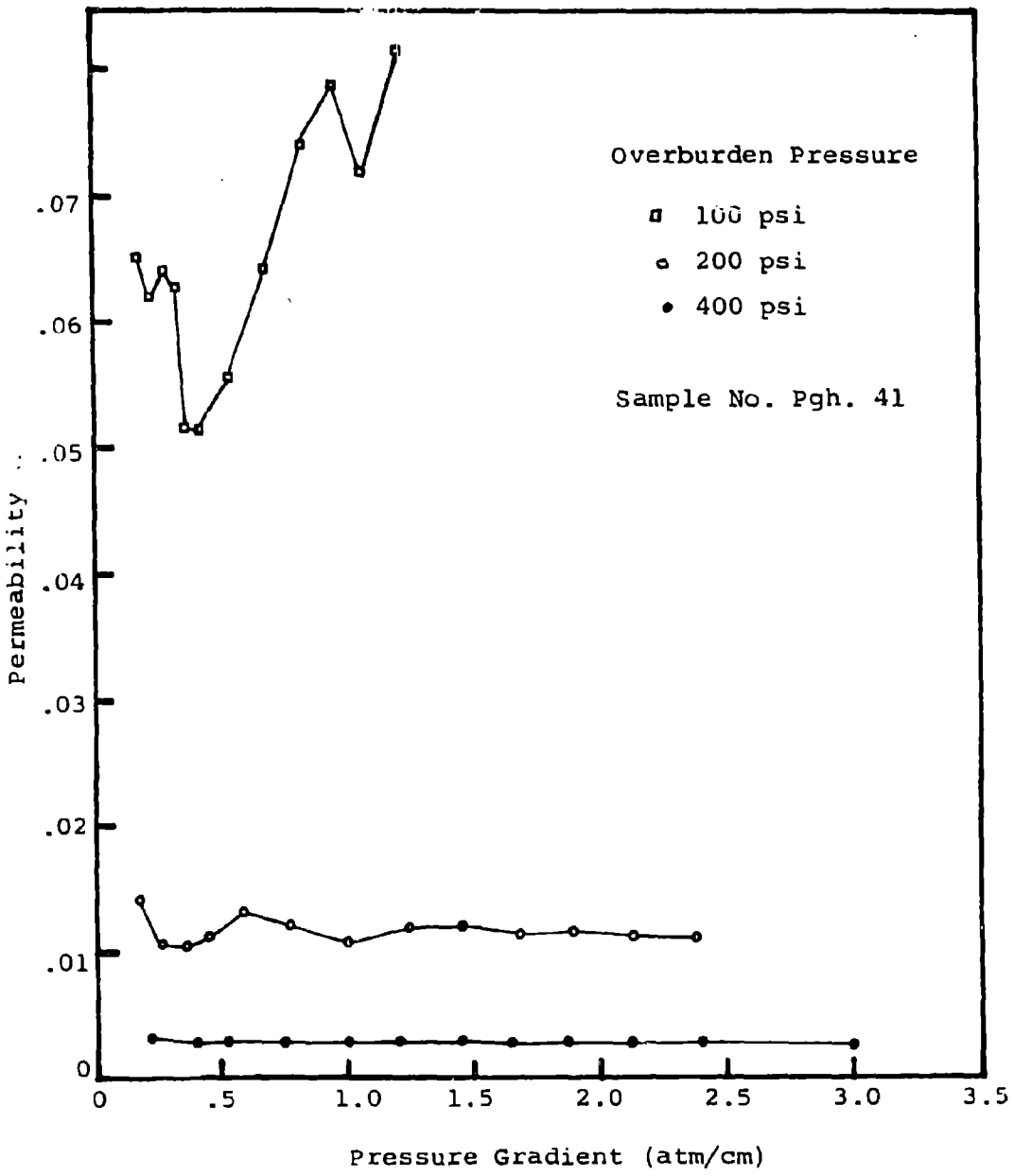

FIGURE 11: PRESSURE PARTING TEST

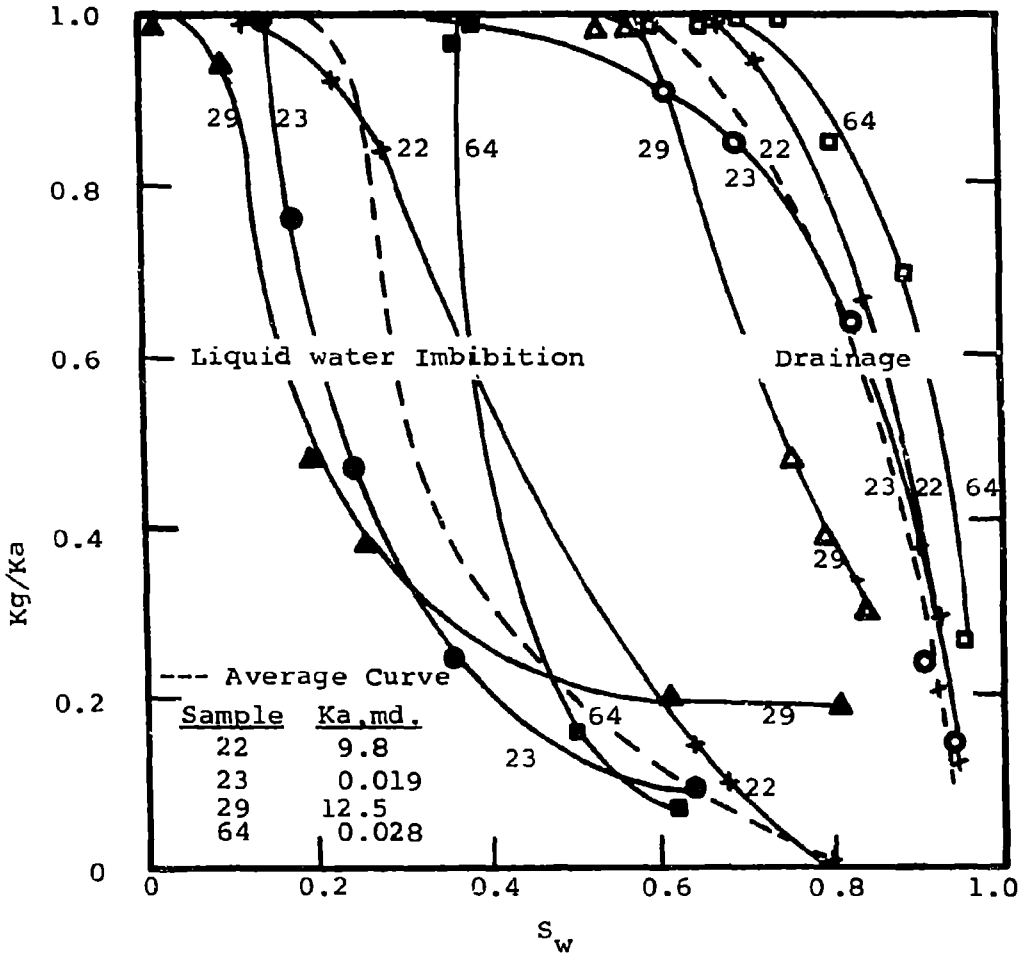

FIGURE 12: DRAINAGE AND IMBIBITION RELATIVE PERMEABILITY CURVES FOR PITTSBURGH COAL

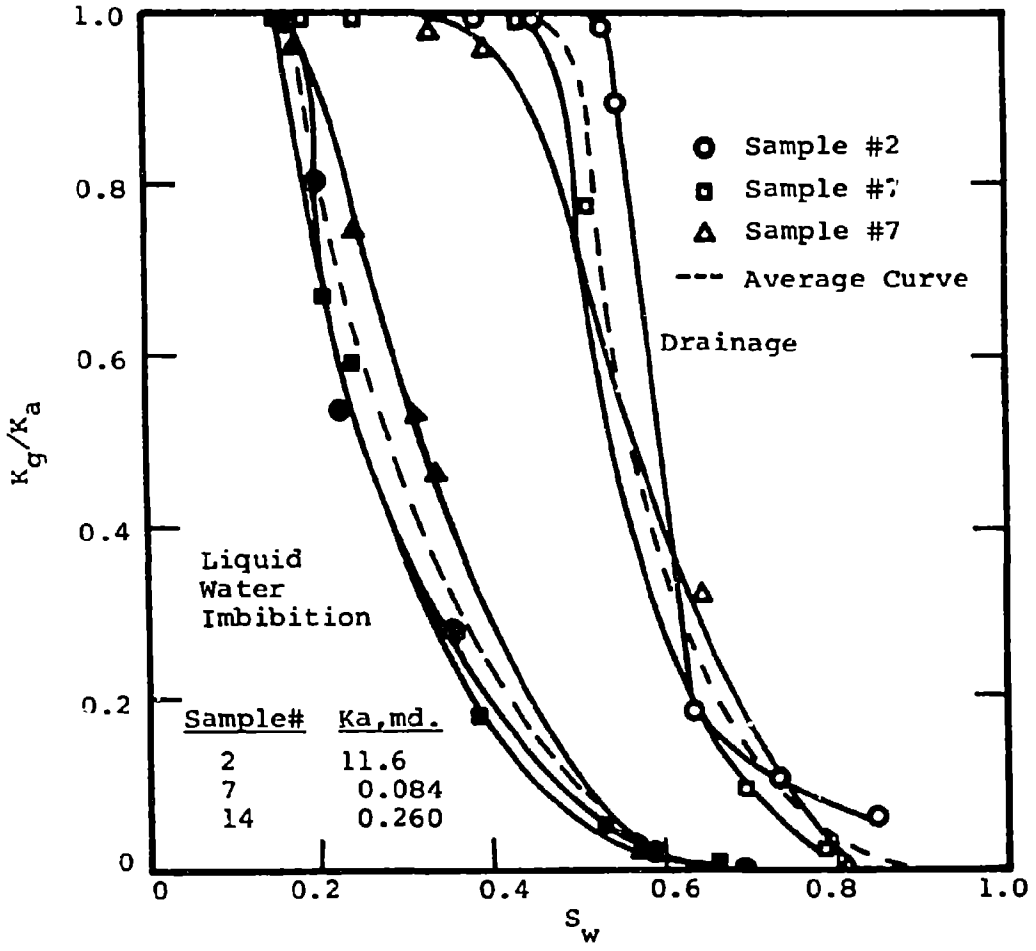

FIGURE 13: DRAINAGE AND IMBIBITION RELATIVE PERMEABILITY CURVES FOR POCAHONTAS COAL

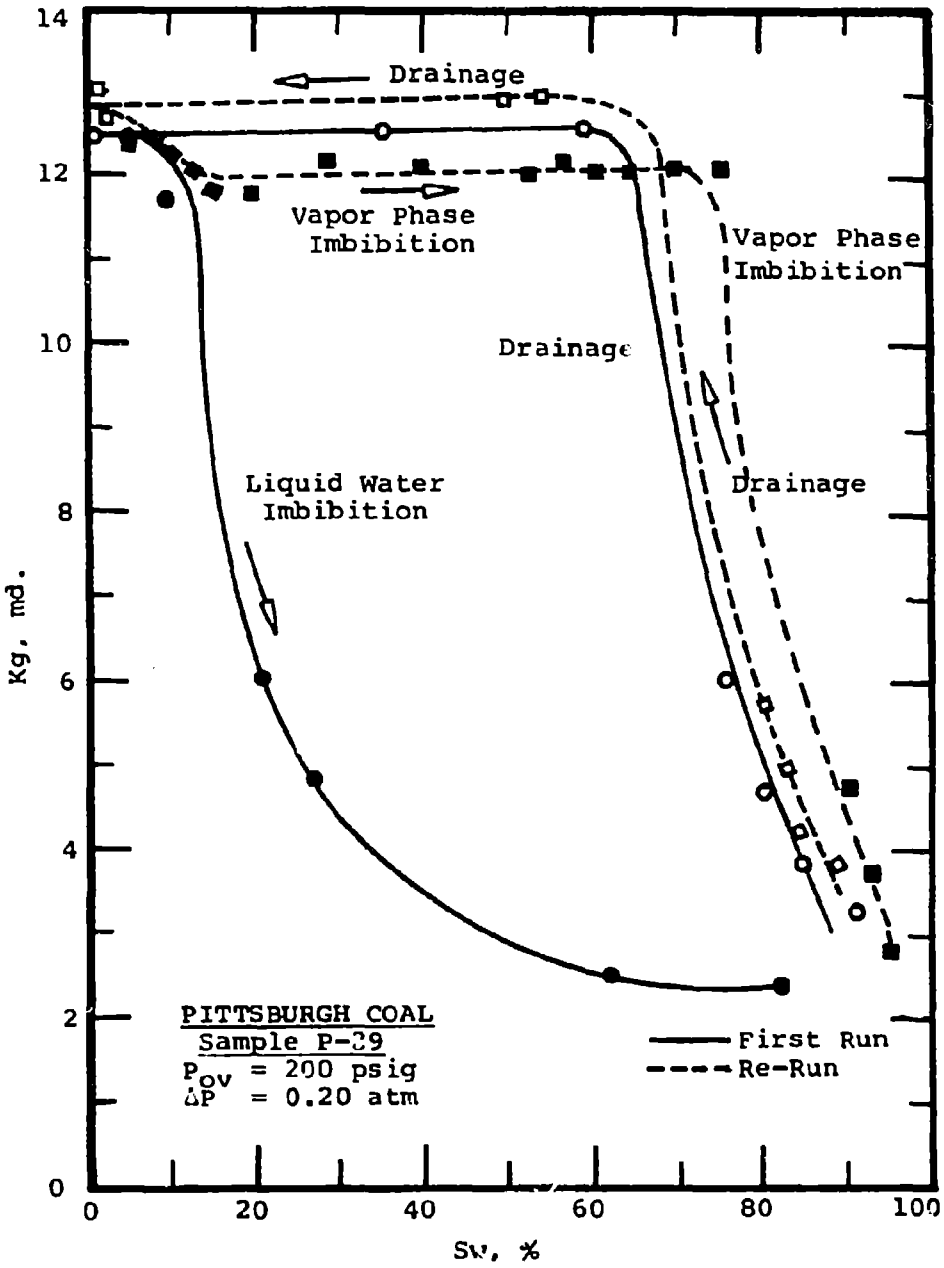

FIGURE 14: EFFECTIVE GAS PERMEABILITY OF COAL, Kg, VS. WATER SATURATION, Sw

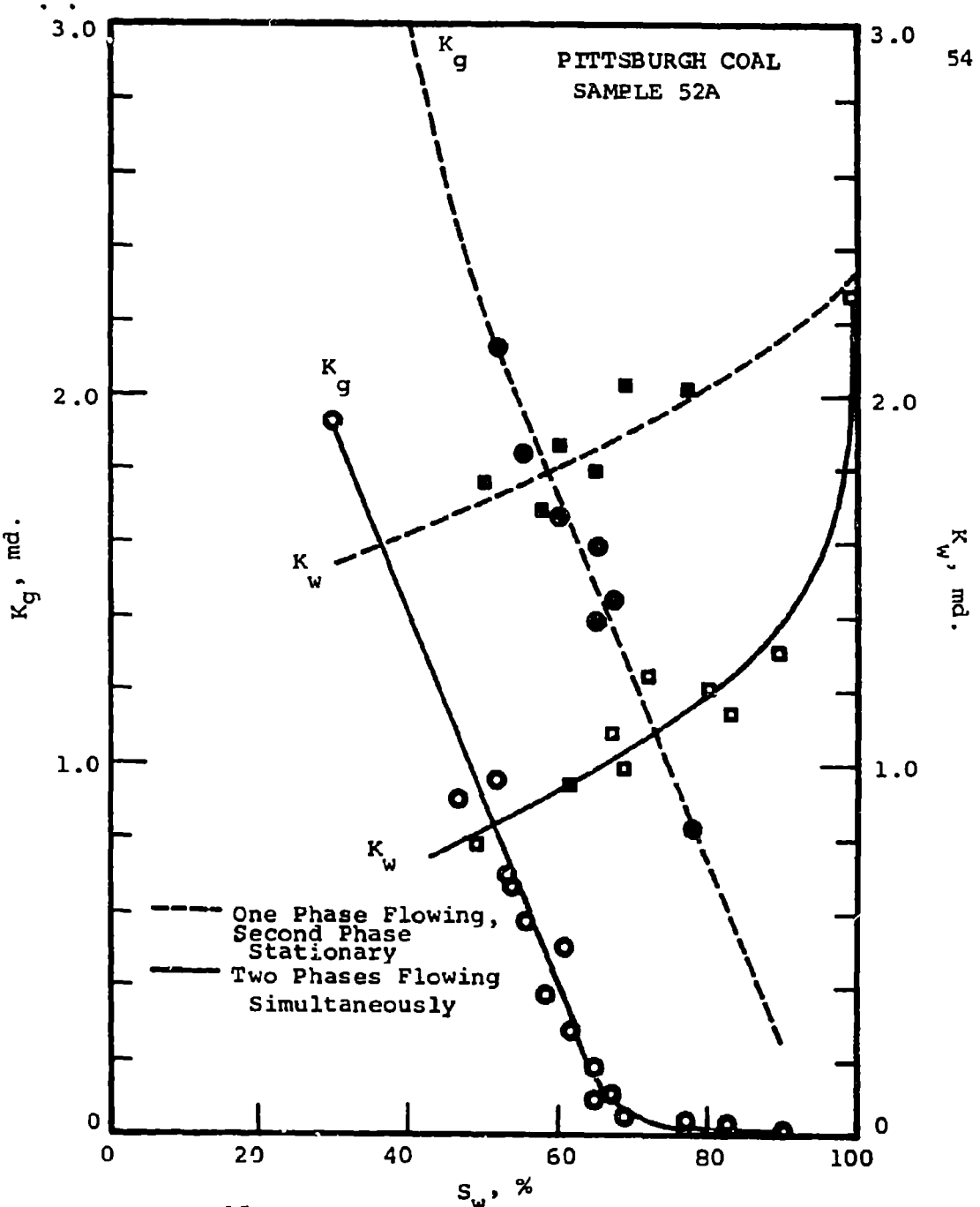

FIGURE 15: EFFECTIVE PERMEABILITIES OF WATER AND GAS, K_w and K_g, VS. WATER SATURATION, S_w

Sample: PGH-2-1; Pittsburgh Coal

Porosity: 1.11% of Bulk Volume

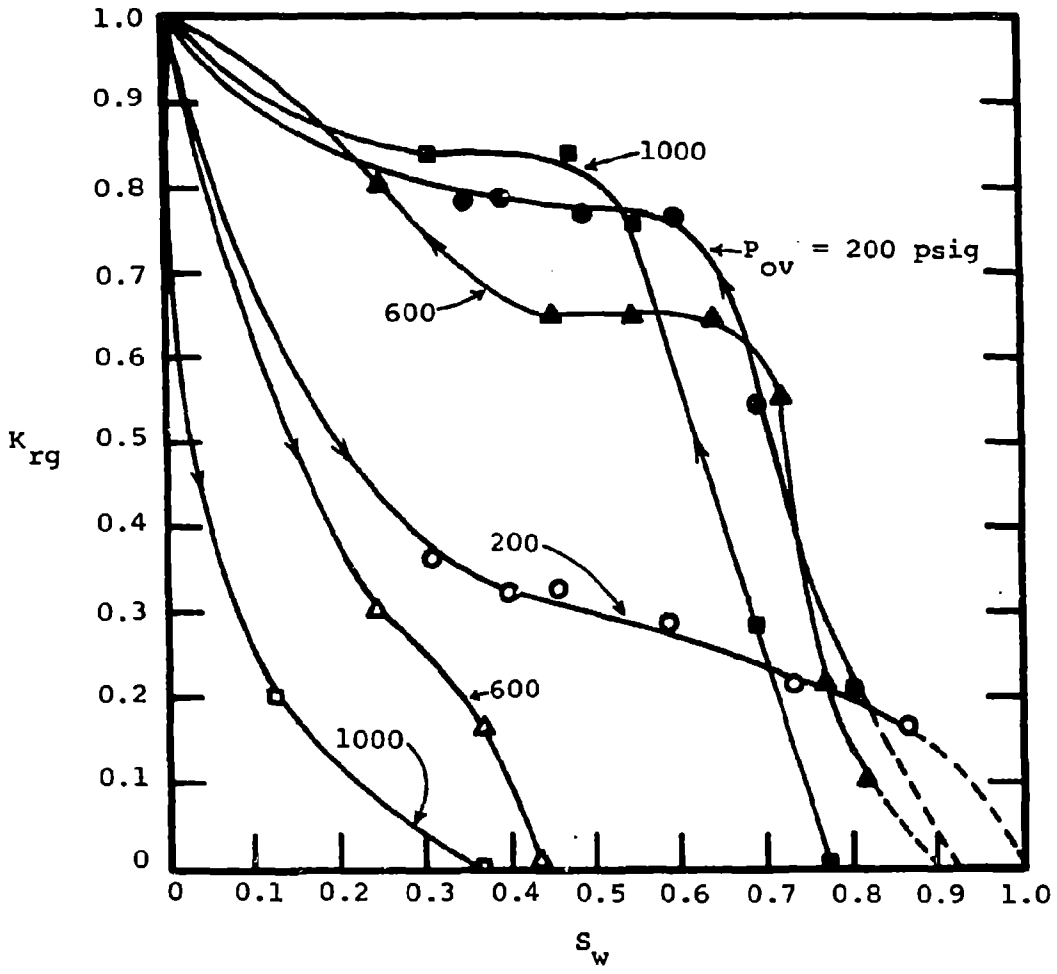

FIGURE 16: RELATIVE PERMEABILITY TO GAS AS A FUNCTION OF WATER SATURATION AND OVERBURDEN PRESSURE

Sample: PGH-2-4; Pittsburgh Coal

Porosity: 4.50% of Bulk Volume

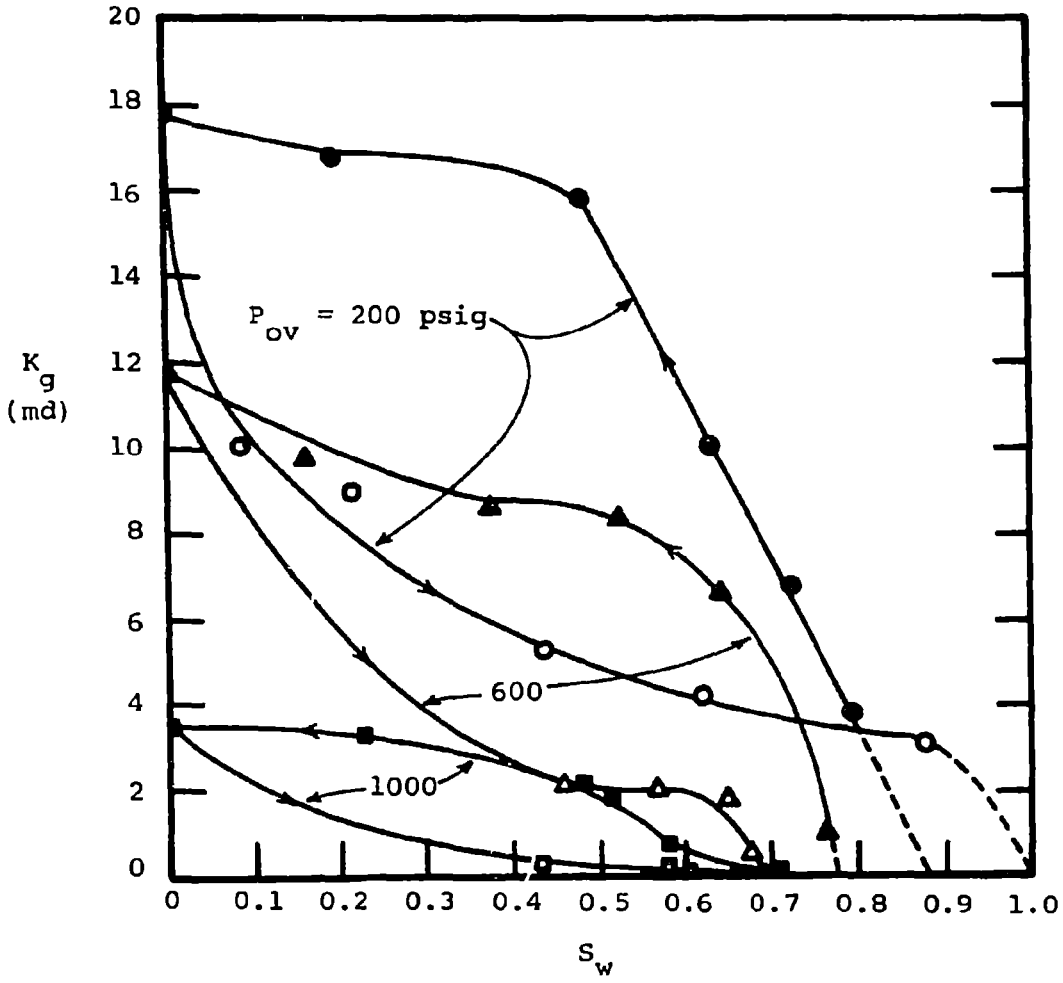

FIGURE 17: EFFECTIVE PERMEABILITY TO GAS AS A FUNCTION OF WATER SATURATION AND OVERBURDEN PRESSURE

Sample: PGH-2-4; Pittsburgh Coal

Porosity: 4.50% of Bulk Volume

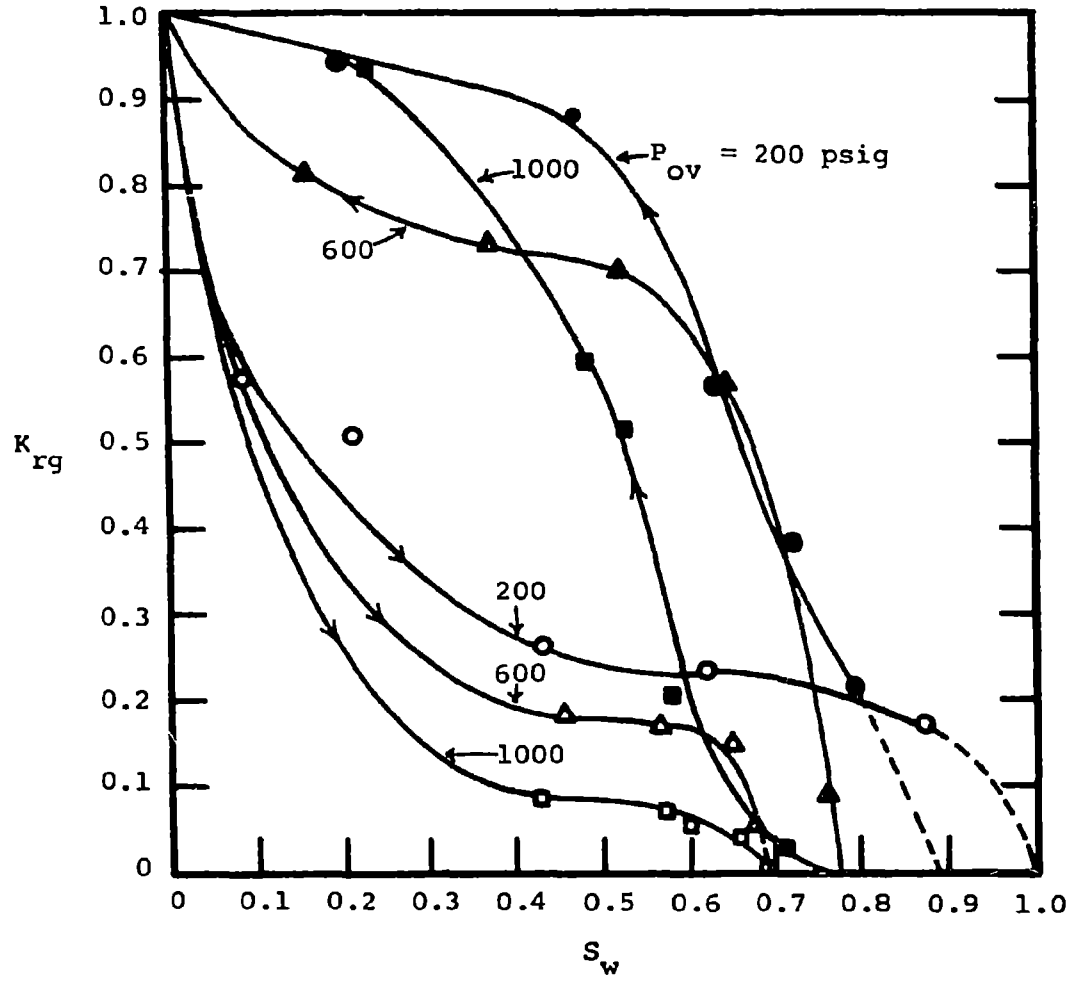

FIGURE 18: RELATIVE PERMEABILITY TO GAS AS A FUNCTION OF WATER SATURATION AND OVERBURDEN PRESSURE

SAMPLE: Poc.-2-3: Pocahontas Coal

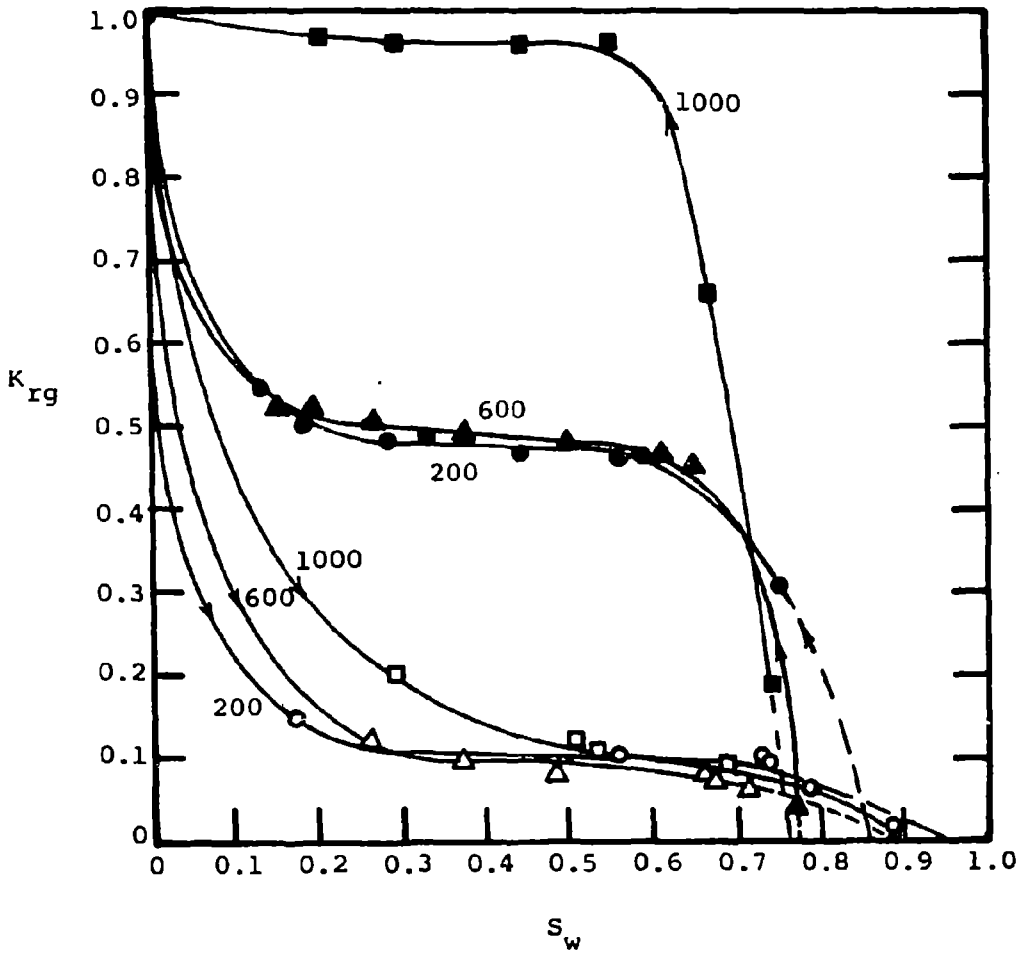

FIGURE 19: RELATIVE PERMEABILITY TO GAS AS A FUNCTION OF WATER SATURATION AND OVERBURDEN PRESSURE

Sample: PGH-2-5; Pittsburgh Coal

Porosity: 3.44% of Bulk Volume

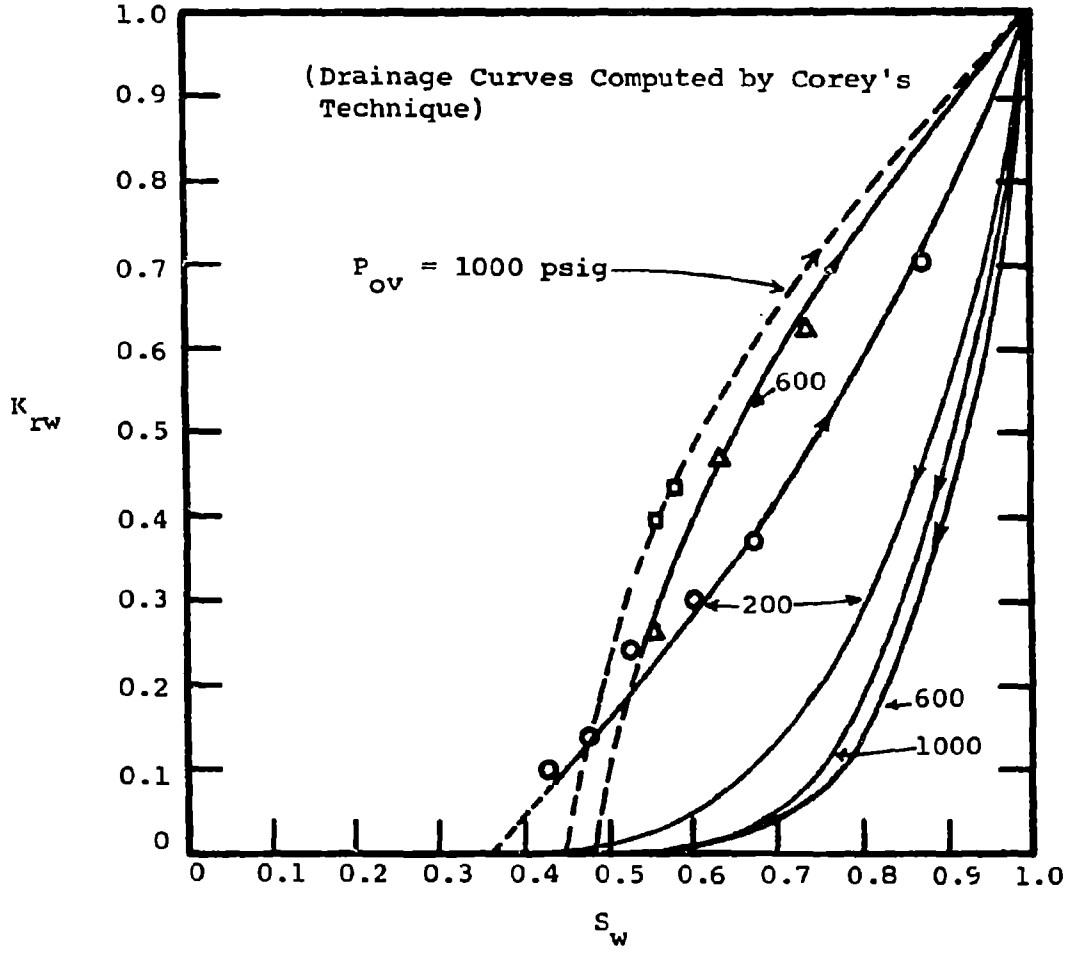

FIGURE 20: RELATIVE PERMEABILITIES TO WATER AS A FUNCTION OF WATER SATURATION AND OVERBURDEN PRESSURE

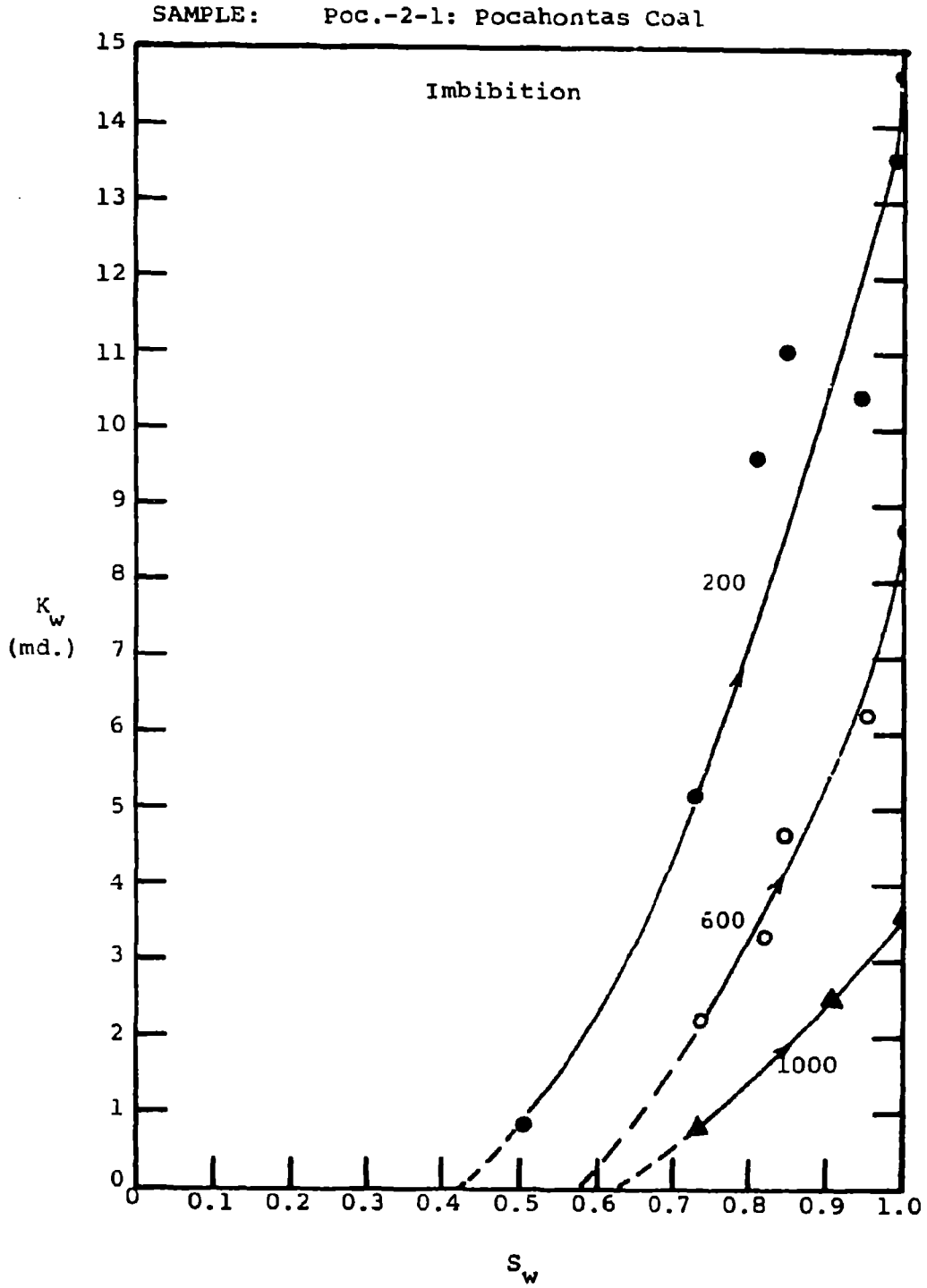

FIGURE 21: EFFECTIVE PERMEABILITY TO WATER AS A FUNCTION OF WATER SATURATION AND OVERBURDEN PRESSURE

SAMPLE: Poc.-2-1: Pocahontas Coal

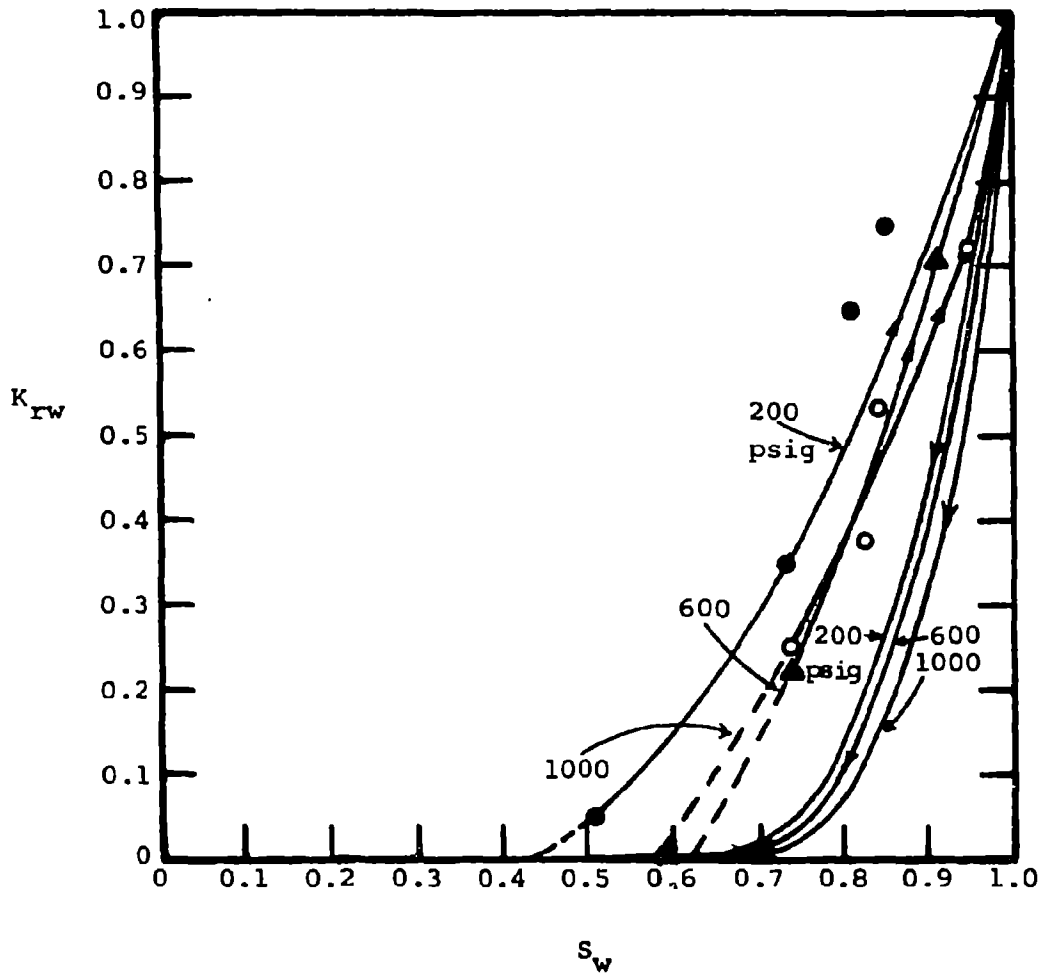

FIGURE 22: RELATIVE PERMEABILITY TO WATER AS A FUNCTION OF WATER SATURATION AND OVERBURDEN PRESSURE

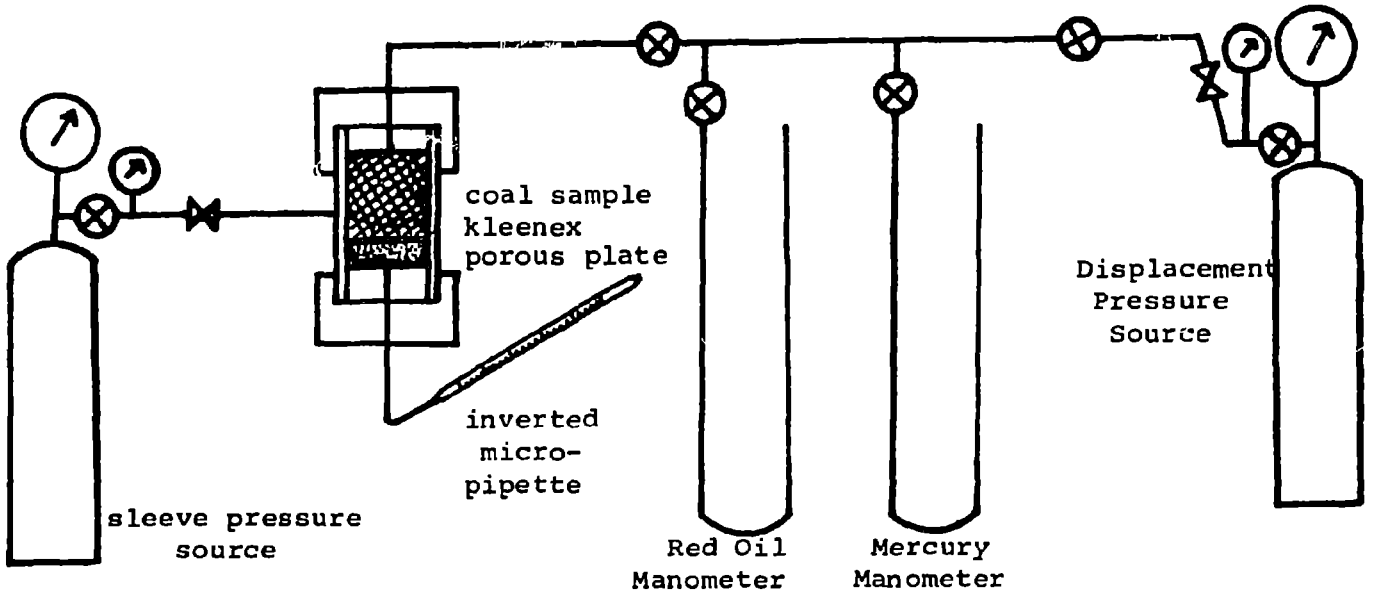

FIGURE 23: EXPERIMENTAL APPARATUS FOR CAPILLARY PRESSURE MEASUREMENTS AT VARIOUS OVERBURDEN PRESSURES

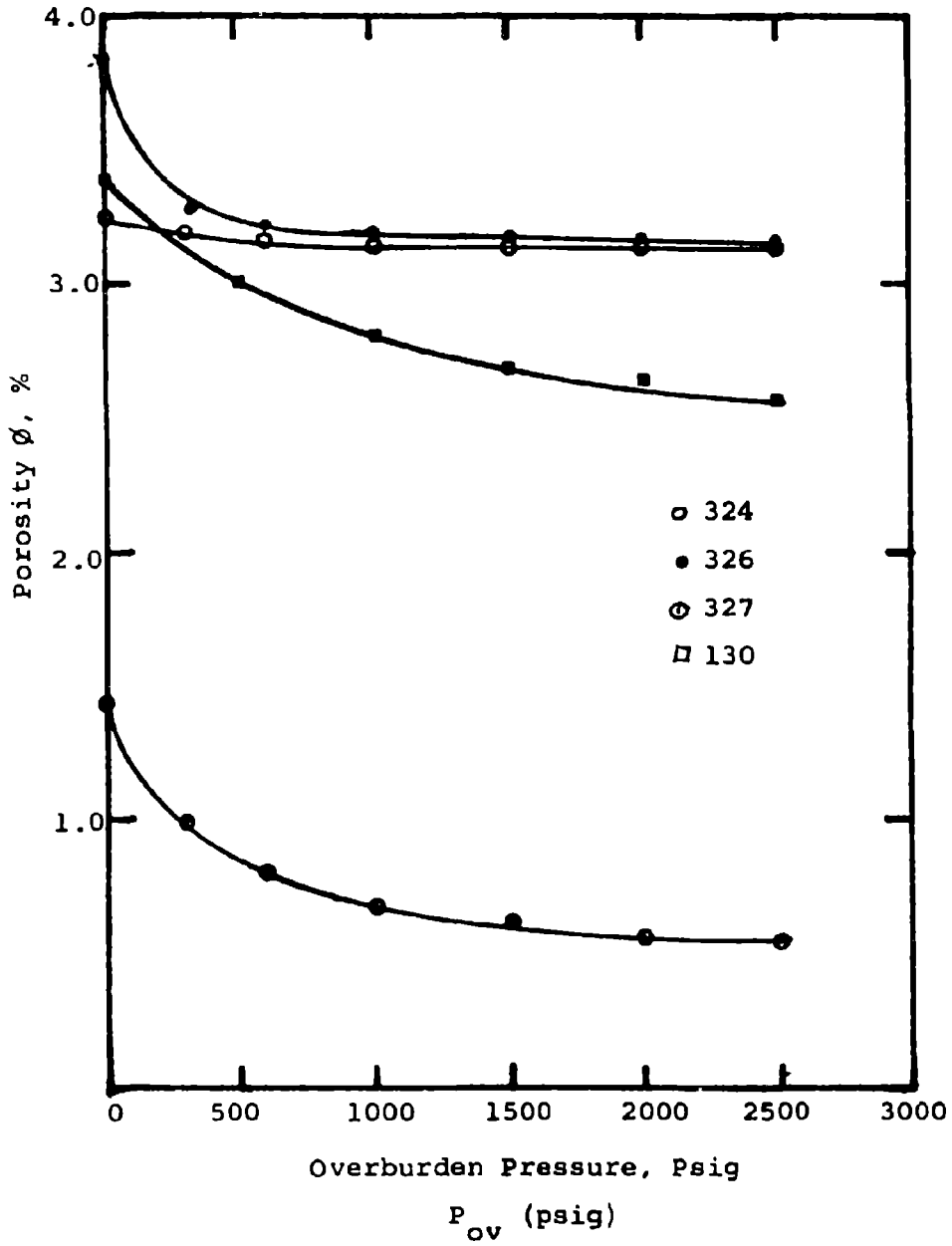

FIGURE 24: PORE COMPRESSIBILITY FOR PITTSBURGH COAL

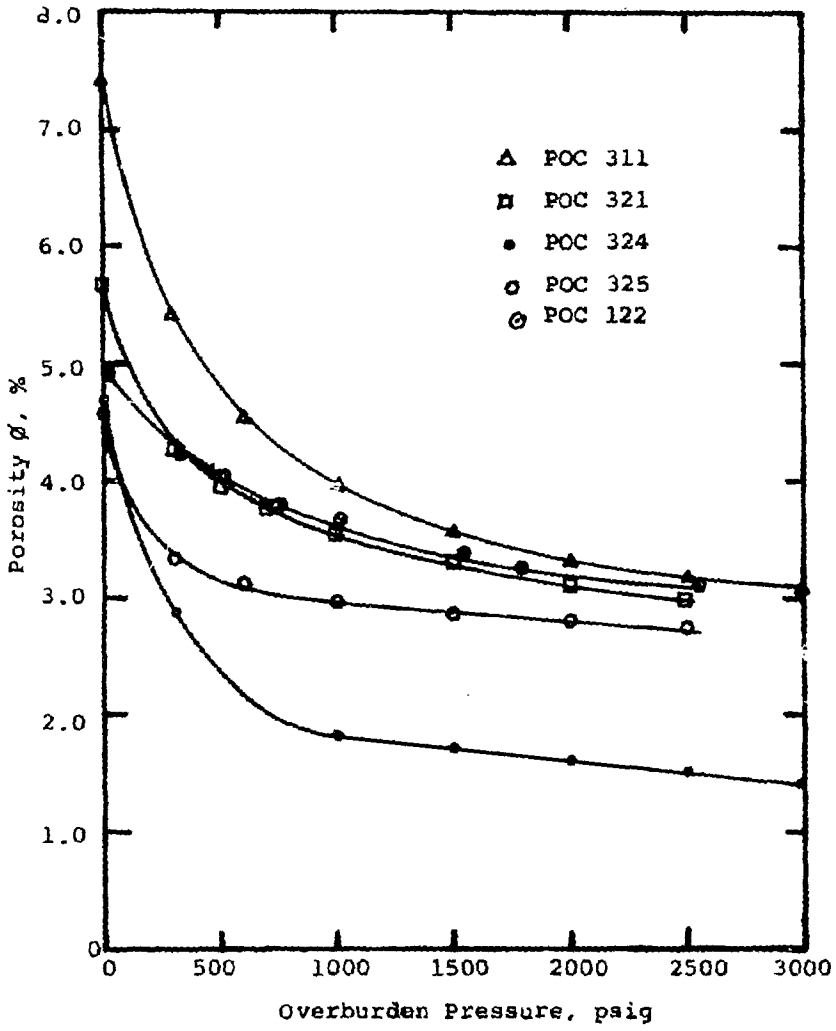

FIGURE 25: PORE COMPRESSIBILITY FOR POCAHONTAS COAL

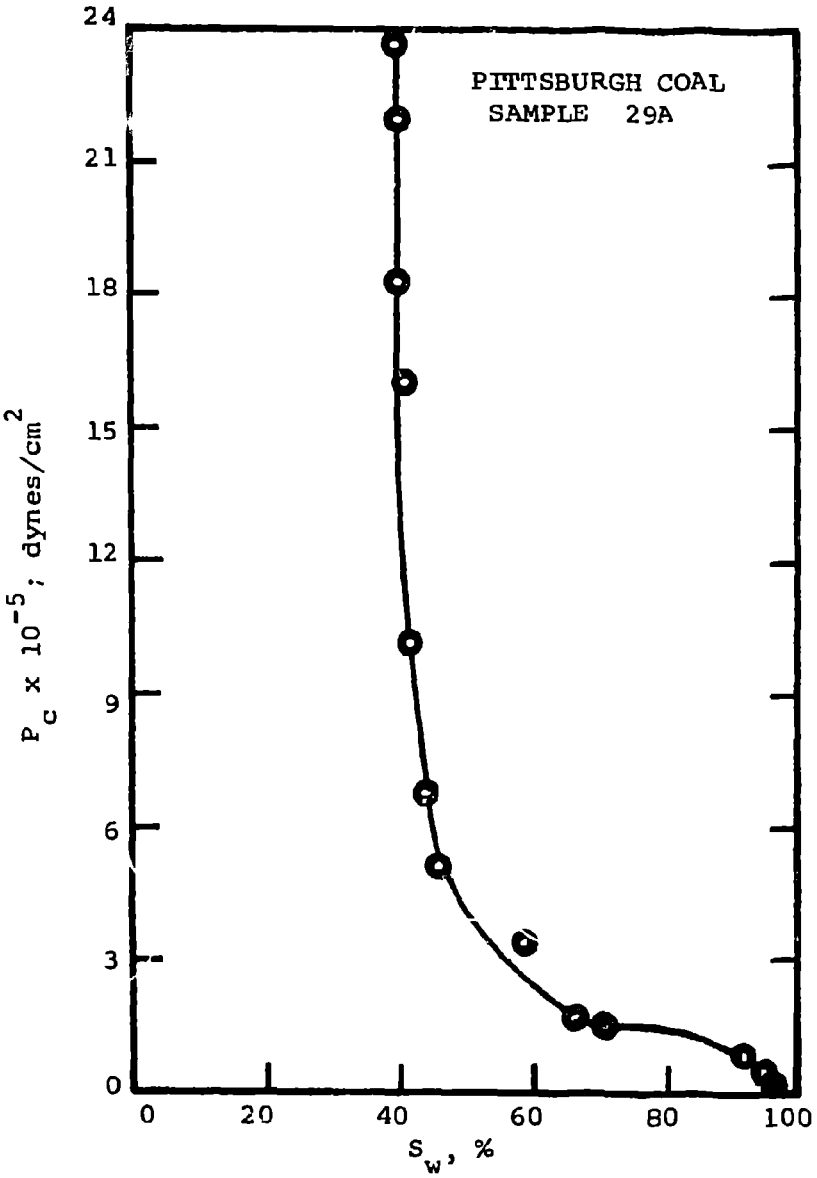

FIGURE 26: CAPILLARY PRESSURE, P_c, VS. WATER SATURATION, S_w

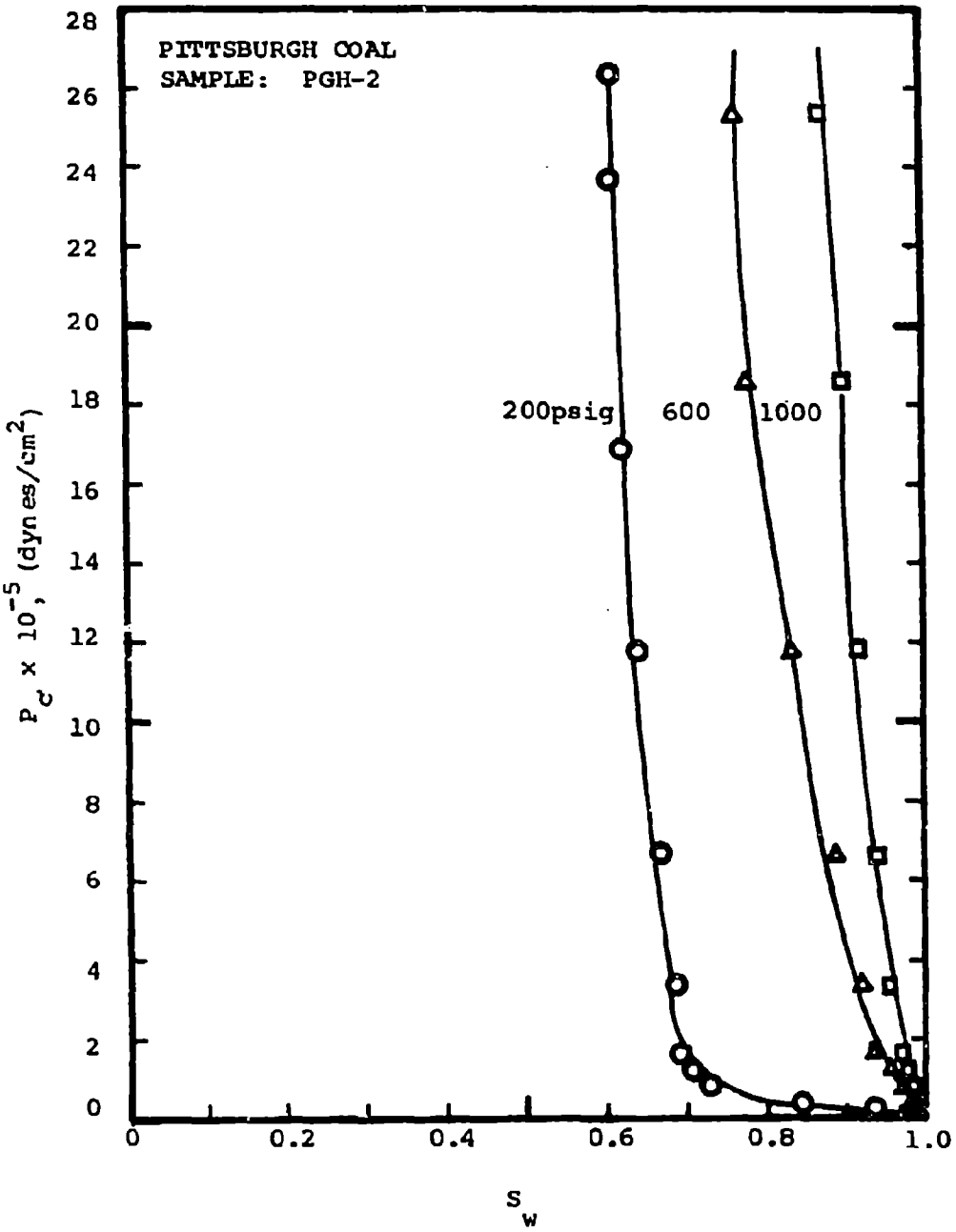

FIGURE 27: CAPILLARY PRESSURE, Pc, vs. WATER SATURATION, S_w, AT VARIOUS OVERBURDEN PRESSURES

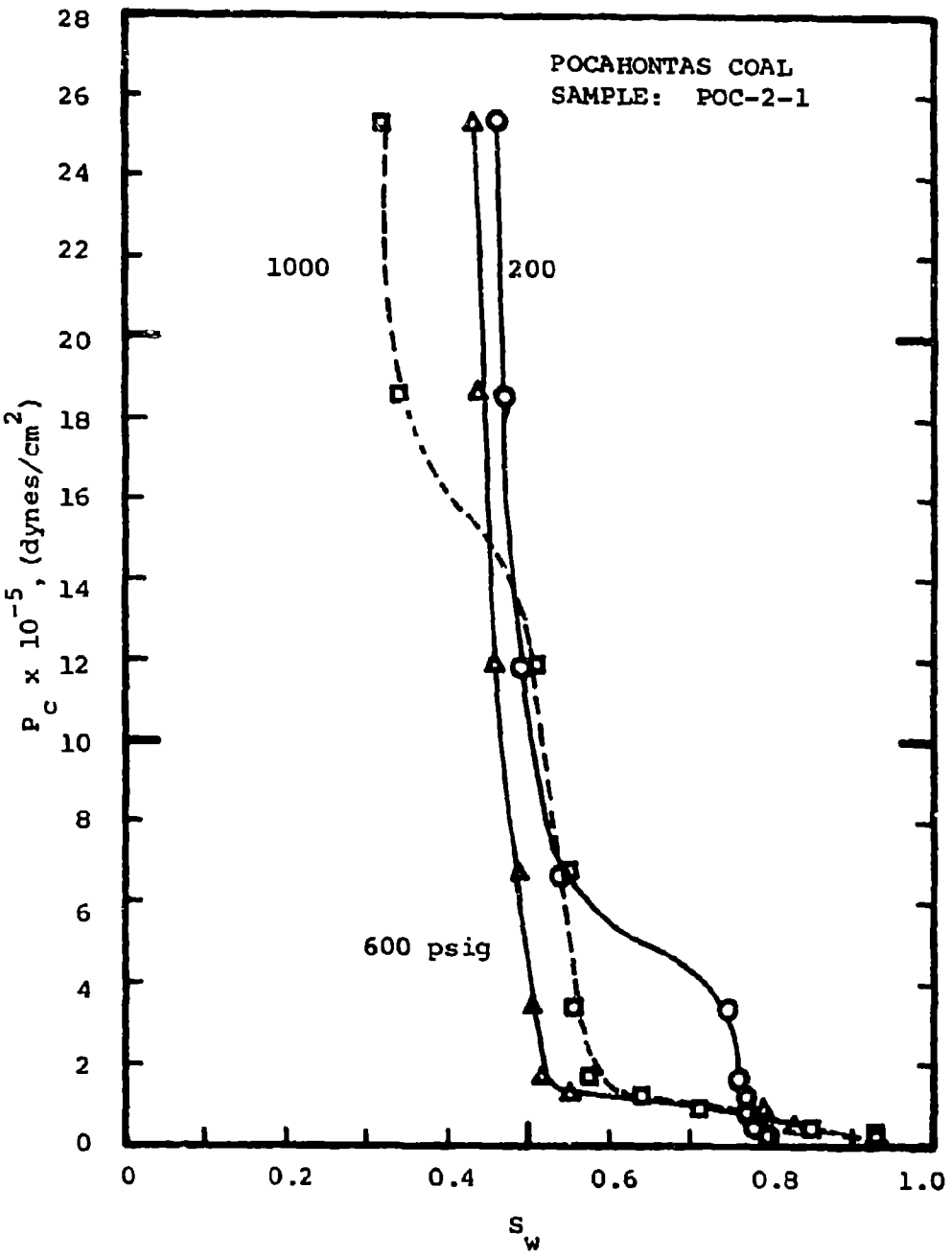

FIGURE 28: CAPILLARY PRESSURE, P_c, vs. WATER SATURATION, S_w, AT VARIOUS OVERBURDEN PRESSURES

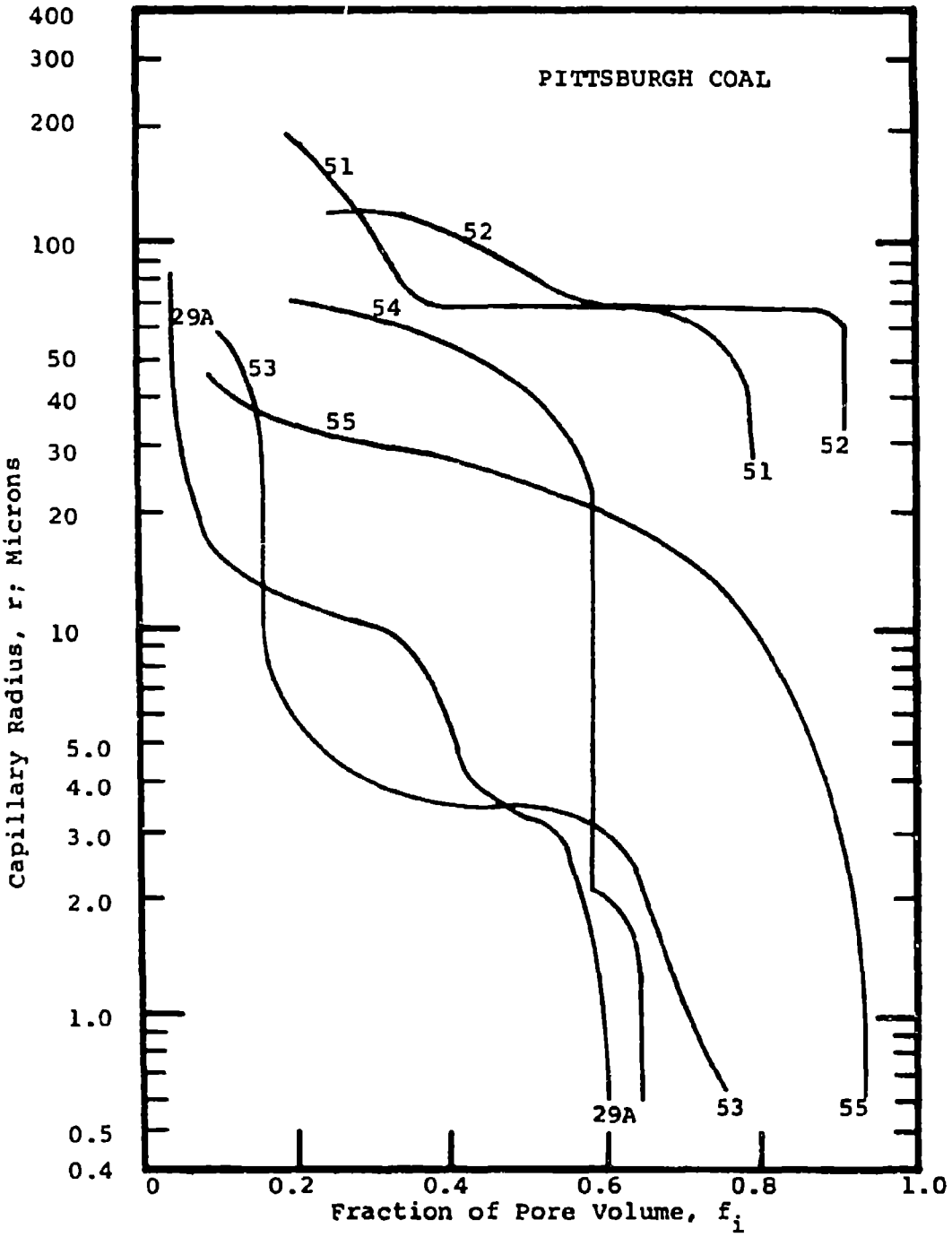

FIGURE 29: PORE SIZE DISTRIBUTION FOR PITTSBURGH COAL SAMPLES

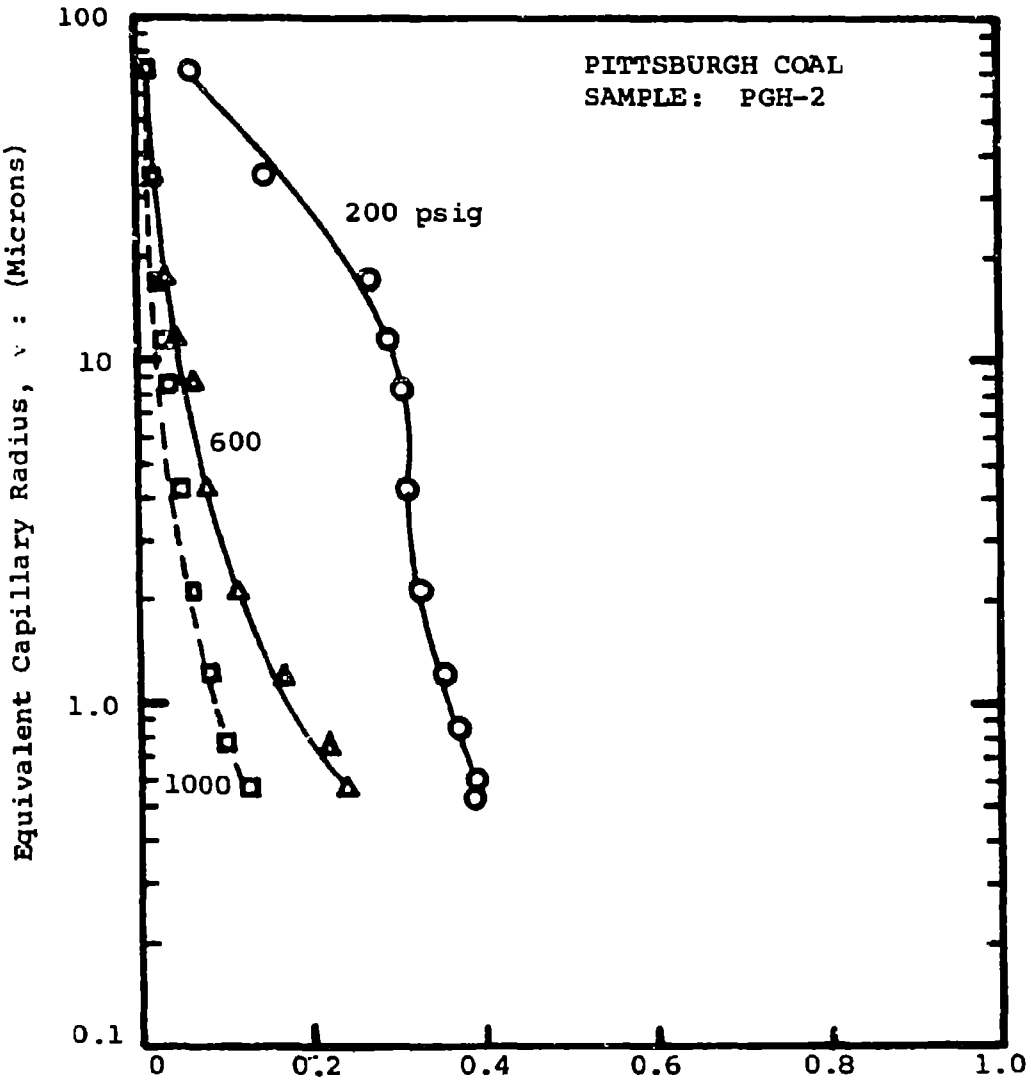

FIGURE 30: CAPILLARY RADIUS, γ, vs. FRACTION OF PORE VOLUME, f_i WITH SIZE EQUAL TO OR GREATER THAN, γ_i AT VARIOUS OVERBURDEN PRESSURES

TABLE 1

THE IMBIBITION OF WATER BY PITTSBURGH COAL

SAMPLE NUMBER C-1

Time (hrs)	Wet Weight (gm)	Gain in Wt. (gm)	Calculated Porosity %
0	0	0	-
1/4	19.8415	0.3101	2.066
2	19.8965	0.3651	2.432
3	19.9175	0.3861	2.572
4	19.9350	0.3936	2.689
4	19.9385	0.4071	2.712
14	19.9775	0.4461	2.972
28	19.9950	0.4536	3.088
38	19.9960	0.4646	3.095
50	20.0131	0.4817	3.209
100	20.0282	0.4968	3.310
160	20.0355	0.5021	3.358
170	20.0392	0.5078	3.383
210	20.0394	0.5080	3.384
220	20.0393	0.5079	3.383

Bulk vol. = 15.011 cc

Dry Wt. = 19.5314 gr.

TABLE 2

ABSOLUTE PERMEABILITY TO AIR OF PITTSBURGH COAL SAMPLES*

Sample	Mean Flow Press. Range Atm.	K_a, md
PGH- 1	1.26 - 2.14	0.12
2	1.04 - 2.16	4.64
3	2.00 - 2.14	0.05
4	1.03 - 2.10	4.02
5	1.24 - 2.14	0.38
6	1.24 - 2.14	0.20
7	1.14 - 1.75	5.14
8	1.04 - 2.14	5.47
9	1.04 - 1.51	44.70
10	1.25 - 2.10	2.80
PGH-11	1.05 - 1.85	21.70
12	2.14	no flow
13	1.24 - 2.10	7.70
14	1.24 - 2.10	0.18
15	2.00 - 2.14	0.054
16	2.14	no flow
17	2.14	no flow
18	1.25 - 2.14	2.30
19	1.05 - 1.85	43.0
20	1.05 - 1.85	16.50
PGH-22	1.14 - 2.14	7.90
23	1.14 - 2.14	11.40
24	2.14	0.035
25	2.14	0.235
26	2.14	no flow
27	2.14	<0.01
28	2.14	<0.01
29		12.50
30		6.90
PGH-41		2.90
52		9.0
53		13.0
61		2.4
63		4.8
64		0.03

*Confining Pressure = 200 psig

TABLE 3

ABSOLUTE PERMEABILITY DISTRIBUTION FOR PITTSBURGH AND POCAHONTAS COALS

Perm. Range md	Fractional Distribution		
	Pittsburgh Coal	Pocahontas Coal	
	P_{con} = 200 psig	P_{con} = 200 psig	P_{con} = 400 psig
> 100	----	0.04	----
10 - 100	0.20	0.11	0.07
1 - 10	0.37	0.21	0.20
0.1 - 1	0.14	0.60	0.64
0.01 - 0.1	0.12	0.04	0.07
< 0.01	0.17	----	0.02
	1.00	1.00	1.00

TABLE 4

COMPARISON OF PERMEABILITIES OF COAL SAMPLES MEASURED AT ONE ATMOSPHERE TO THE VALUES OBTAINED BY EXTRAPOLATION TO INFINITE MEAN FLOW PRESSURES

Sample	K_1 atm md.	K_∞ md	% Reduction in Permeability
PGH- 4	4.5	4.0	11.2
6	0.43	0.20	46.5
10	5.3	2.7	49.0
13	8.6	7.7	10.4
14	0.60	0.20	66.7
15	0.062	0.054	12.9
18	2.85	2.30	19.3
18*	1.80	1.60	11.1
19	49.0	43.0	12.2
19**	45.5	42.5	6.7
20	19.2	16.5	14.0

*Moisture Content: 1.29% by Weight

**Moisture Content: 0.98% by Weight

TABLE 5

POCAHONTAS COAL PERMEABILITY TO AIR AT VARIOUS CONFINING PRESSURES

Sample	K(200),md	K(400),md	K(1600),md	REMARKS
1	.86 .56	.63	.04	3 stress cycles
2	14.70 4.10	9.20	1.60	3 stress cycles
2	1.37 .85	.88	.35	pre-stressed cycle #1
2	.84 .79	.67	.33	pre-stressed cycle #2
3	21.60 2.40	8.10	.00	3 stress cycles
3	1.64 .76	.81	.21	pre-stressed cycle #1
3	.76 .69	.56	.09	pre-stressed cycle #2
3	6.97 2.78	3.04	.00	pre-stressed re-run
5	104.00 26.80	47.30	.00	fresh sample 1 cycle
7	.145 .102	.12	.003	fresh sample 1 cycle
14	.52 .23	.31	.02	pre-stressed 1 cycle (re-run)
14	.967 .10	.176 .10	.024	fresh sample 1 cycle
16	.379 .158	.231	0.67	fresh sample 1 cycle
16	.294 .168	.168	0.67	pre-stressed

TABLE 6

WATER PERMEABILITY OF PITTSBURGH AND POCAHONTAS COAL SAMPLES

Sample	Dry Wt. gr.	Saturated Wt. gr.	Water Content at 100% S_w, gr	S_w Initial	S_w Final	S_w Average	K_{air} md	K_{water} md
			Pittsburgh Coal					
61	40.045	40.345	.300				2.4	.069
62	42.140	42.866	.746				357.	167.
63a	58.839	59.765	.926	1.0	1.0	1.0	4.8	2.0
63b	58.839	59.765	.926	1.0	1.0	1.0	4.8	1.48
63c	58.839	59.765	.926	1.0	.84	.92	4.8	.79
63d	58.839	59.765	.926	1.0	.90	.95	4.8	1.05*
52a	50.700	51.394	.707	1.0	.89	.95	9.0	4.86
52b	50.700	51.394	.707	.98	.87	.93	9.0	2.41
52c	50.700	51.394	.707	.93	.91	.92	9.0	1.90
52d	50.700	51.394	.707	.95	.91	.93	9.0	1.07
64	37.185	37.435	.250				.03	.09
53		47.478				1.0	13.1	7.61
			Pocahontas Coal					
1	43.292	44.670	.911	.66	1.0	.66	.44	5.3
1b	43.292	44.670	.911	.66	.66	.66	.44	2.31
2a	42.149	43.005	.856				.18	12.3
2b	42.149	43.005	.856	1.0	.95	.98	.18	20.0

TABLE 6
(Continued)

7	48.857	49.568	.711				.08	.08
14	42.922	43.717	.795	1.0	.78	.89	10.0	.82

*Ten days had elapsed after Run "c"

TABLE 7

AIR AND WATER PERMEABILITIES OF COAL SAMPLES AT VARIOUS OVERBURDEN PRESSURES

Sample No.	Coal Formation	Porosity* (% of bulk vol.)	Overburden Pressure (psig)	Permeability to air (md)	Permeability to water (md)
Poc.-2-1	Pocahontas	5.16	199	34.6	14.8
			599	12.3	8.70
			996	9.65	3.60
Poc.-2-2	Pocahontas	4.55	196	18.6	14.4
			596	5.83	5.70
			993	1.59	1.80
Poc.-2-3	Pocahontas	4.31	200	275	62.4
			600	19.5	20.3
			993	3.07	3.02
Poc.-2-4	Pocahontas	3.73	196	14.9	7.90
			596	3.10	2.56
			968	0.760	0.455
Pgh.-2-6	Pittsburgh	1.82	193	2.24	1.25
			593	0.814	0.547
			968	0.274	0.098

*Porosities determined at zero overburden pressure.

TABLE 8

POROSITY OF COAL SAMPLES FROM THE PITTSBURGH SEAM

					One Hour Saturation Time		Ten Hour Saturation Time	
ample No.	Air Permeability md.	Bulk Vol., cc.	Helium Pore Vol., cc.	Helium Porosity %	Water Pore Vol., cc.	Water Porosity cc.	Water Pore Vol., cc.	Water Porosity %
P-1	0.12	14.775	0.7240	4.900	0.0471	0.319	0.0622	0.421
P-4	4.72	15.3720	0.3979	2.586	0.0706	0.459	0.0936	0.609
P-5	0.38	8.233	0.7104	8.628	0.0684	0.831	0.0905	1.094
P-6	0.33	10.605	0.5272	4.971	----	---	0.0784	0.739
P-8	5.47	9.142	0.2876	3.145	----	---	0.0575	0.629

TABLE 9

POROSITY VALUES FOR AIR-DRIED AND OVEN-DRIED COAL SAMPLES

Sample Number	Air Dried		Oven Dried	
	He Porosity %	Water Porosity %	He Porosity %	Water Porosity %
A-1	2.358	0.313	2.610	0.379
A-2	4.408	0.344	4.463	0.60
B-1	8.950	0.408	12.388	1.405

TABLE 10

Sample	Overburden Pressure psig	Porosity, Ø % Atmospheric	Porosity, Ø % at overburden	Air Perm., Ka md at overburden
PGH 2-a	200	2.02	1.71	3.1
b	600	2.28	1.94	1.66
c	1000	2.61	2.01	0.47
PGH 25-a	200	2.04	1.77	823.22
b	600	2.16	0.86	105.72
c	1000	2.23	1.63	290.69
PGH 26-a	200	3.05	2.76	22.22
b	600	3.45	3.27	4.69
c	1000	3.46	2.58	2.54
POC 2-1-a	200	5.35	4.81	13.0
b	600	5.42	5.21	5.65
c	1000	5.27	4.88	3.79
POC 2-2-a	200	4.41	3.92	7.39
b	600	4.57	4.14	2.93
c	1000	4.65	4.25	1.68